A Toolkit for automated High-Throughput Cloning and Manipulation of DNA in Fission and Budding yeast

Devina Singh

A

Thesis

In the

Department of Biology

Presented in Partial Fulfillment of the Requirements for the Degree of

Master of Science (Biology)

at

Concordia University
Montreal, Quebec, Canada

December 2022

CONCORDIA UNIVERSITY
School of Graduate Studies

This is to certify that the thesis is prepared

By: **Devina Singh**

Entitled: **A Toolkit for automated high-throughput cloning and manipulation of DNA in fission and budding yeast**

And submitted in partial fulfillment of the requirements for the degree of

Master of Science (Biology)

Complies with the regulations of the university and meets the accepted standards with respect to originality and quality.

Signed by the final Examining Committee:

_____ Chair
Dr. Malcolm Whiteway

_____ Examiner
Dr. Laurent Potvin-Trottier

_____ Examiner
Dr. Malcolm Whiteway

_____ Examiner
Dr. Paul Joyce

_____ Supervisor
Dr. Aashiq Kachroo

Approved by

_____ Graduate Program Director
Dr. Robert Weladji

_____ Dean of Faculty
Dr. Pascale Sicotte
2022/2023

Abstract

A Toolkit for Automated High-Throughput Cloning and Manipulation of DNA in Fission and Budding yeast

Devina Singh

Budding and fission yeast continue to serve as outstanding models for biomedical research. However, while budding yeast is emerging as a model eukaryote for synthetic biology with many readily available fully-characterized toolkits, fission yeast has lagged partly due to the lack of similar resources. Furthermore, the development of genome foundries demands compatible platforms that enable modular, multi-part cloning with precision. Here, we present toolkits combining the Gateway and Golden Gate technologies for precise, automated, high-throughput cloning and genome engineering for both yeasts.

For budding yeast, we modified a previously available toolkit into robotics-compatible vectors. For fission yeast, this platform provides a new set of vectors for modular assemblies, including a fully characterized collection of promoters and terminators. Additionally, we engineered a non-toxic, codon-optimized, genome-editing tool for efficient modifications of the fission yeast genome. Finally, we show the utility of the toolkit for precision cloning and the expression of heterologous human proteins in yeast.

Acknowledgements

I would like to thank my supervisor Dr. Aashiq Kachroo for supporting this work and the never ending patience he demonstrated while providing guidance and mentorship throughout the project. I want to extend my gratitude towards my colleagues who have supported, assisted and provided me with invaluable tips and guidance as well as encouragement throughout my degree. Thank you to Brittany Greco, Mudabir Abdullah, Farhat Zafar, Michelle Vandeloo, Dr. Jeffery Bouffard, Christian Dykstra, Tom Kazmirchuk, Dr. Mohammed Nasr, Sophie Albert, Aaliya Naaz and Homin Jeong and Yuxiang Ren.

I would also like to thank Dr. Chris Law at the Center for Microscopy and Cellular Imaging at Concordia for training and guidance; Annie Gosselin from the Flow Cytometry Core Facility at IRIC - Institute for Research in Immunology and Cancer in Université de Montréal and Dr J. Boeke for providing me with fission yeast strains and plasmids to begin this work. I would also like to sincerely thank Dr. Smita Amarnath, for her invaluable teachings and aid throughout my degree.

Most importantly, I would like to thank my family for supporting my decision to pursue graduate studies. I am grateful for the determination and perseverance they have instilled in me, as well as for providing me with all the tools I would need to make it to the end of my degree.

Contribution of Authors

This project was conceived by Dr. Aashiq Kachroo. The creation and design of Sc-RoboClo were by Dr. Smita Amarnath. Dr. Smita Amarnath also designed and performed the high-precision assay validating the cloning of RoboClo.

Table of Contents

List of Figures

List of Tables

List of Abbreviations

ARS1: Autonomous Replicating Sequence
MoClo-YTK: Modular Cloning Yeast Tool Kit
DSB: Double-Stranded Breaks
CAS: CRISPR-associated protein
CRISPR: Clustered Regularly Interspaced Short Palindromic Repeats
dCAS9: dead/deactivated Cas9
DNA: Deoxyribonucleic acid
EGFP: enhanced green fluorescent protein
FACS: Fluorescence activated cell sorting
FDA: Food and Drug Administration
gRNA: guide RNA
HDR: Homology-directed recombination
Human ORFeome: Human Open Reading Frame
IDT: Integrated DNA Technologies
IRIC: Institute for Research in Immunology and Cancer
NEB: New England Biolabs
NHEJ: non-homologous end joining
O.D.: Optical Density
PCR: Polymerase Chain Reaction
PADH1: promoter Alcohol dehydrogenase 1A
PCCW12: promoter Cell wall mannoprotein
PENO101: promoter enolase
PGPD3: promoter glyceraldehyde-3-phosphate dehydrogenase
PMG: Pombe Minimal Glutamate
SCRC: *S.cerevisiae* Robo-Clo
SPCO: *S.pombe* Codon-Optimized
SPRC: *S.pombe* Robo-Clo
SPTK: *S.pombe* Tool Kit

1. Chapter 1- Introduction

1.1 The impact of modular toolkits in systematic functional genomic assays in yeast

Production of genetic toolkits has coincided with the rapid progress of synthetic and systems biology research[1,2]. These toolkits consist of basic cloning vectors, expression vectors, part vectors, and CRISPR-Cas9 genome editing systems [2]. Other kits provide vectors carrying parts such as a fully characterized set of promoters, N- or C-terminal tags, and selection markers that are instrumental for performing assays in molecular biology research for budding and fission yeast[3–5]. Due to the readily available collections such as the Human ORFeome, there is a continued need for next-generation high throughput assays that use compatible toolkits offering high precision cloning for both yeasts. Current high throughput DNA assembly technologies use Type IIS restriction systems (Golden Gate) and Gateway cloning[6–8]. For example, the MoClo-YTK kit leverages the Golden Gate strategy, consisting of 96 vectors and several fully characterized yeast promoters, terminators, selection markers, fusion tags, and Cas9-gRNA expression modules[6] (**Figure 1A**). Similar kits have accelerated yeast genetics research by providing the benefit of reliable assemblies of multiple genetic parts such as promoters, genes, and terminators [2,6]. Gateway cloning **(Figure 1B)** collections allow heterologous expression of human genes (from the Human ORFeome collection) into compatible yeast vectors using site-specific recombination [9] [10]. Several other toolkits, such as BioBrick, GoldenBraid, and YeastFab, use similar modular strategies for the highly efficient construction of vectors with unique payloads [2,11–13].

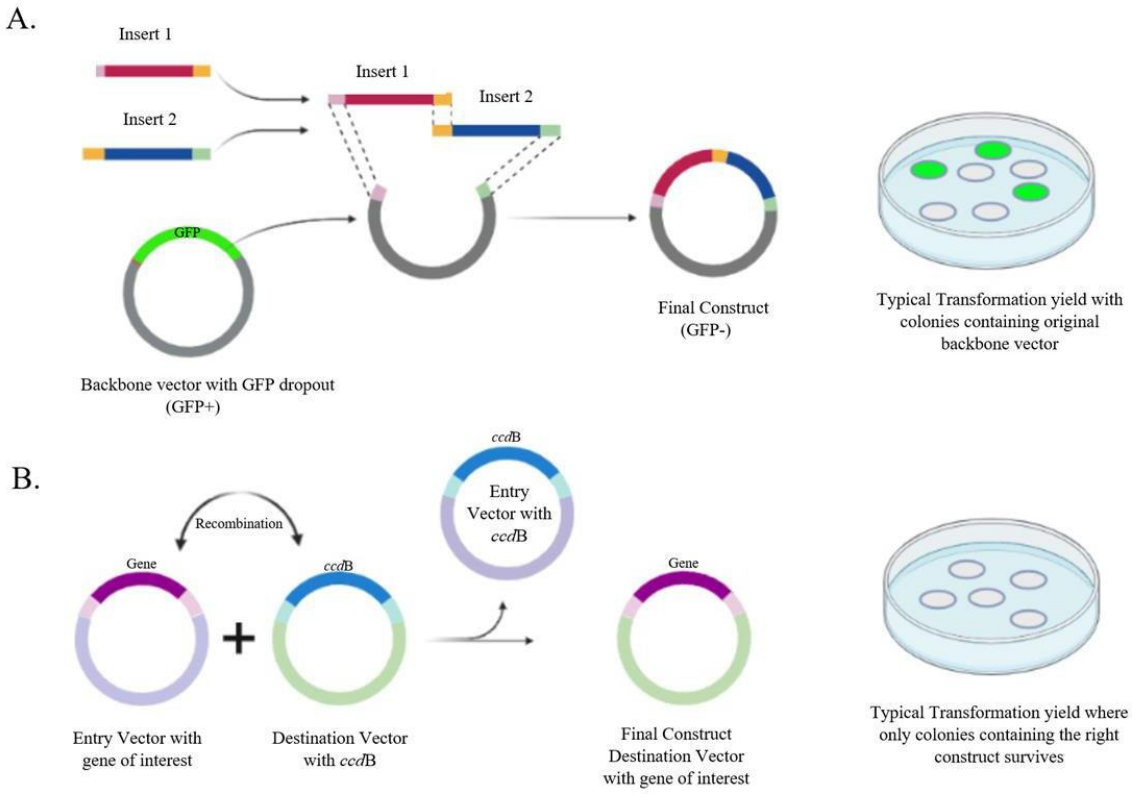

Figure 1. Golden Gate and Gateway Assembly A.*The Golden Gate method involves restriction digestion and ligation of DNA fragments into a fluorescent dropout vector. The final construct is screened by isolating GFP- colonies on a plate which is not ideal in a 96 well format.* ***B.*** *Gateway cloning uses recombination to swap out the gene of interest into the destination vector that contains a toxic ccdB dropout. The toxic cassette eliminates colonies with the wrong backbone, leaving only the correct final construct to survive.*

Over a few decades, budding yeast has emerged as a platform for systems and synthetic biology research demanding high throughput toolkits for genome-wide studies [14]. Modular assembly kits are instrumental in developing novel methods in *S. cerevisiae*. For example, highly optimized yeast two-hybrid systems used MoClo-YTK to create yeast as a drug discovery platform [15]. In particular, our lab focuses on the systematic expression and characterization of human genes in yeast[10,16]. Recent systematic assays using high throughput toolkits and arrayed yeast knockout libraries demonstrated that many conserved genes have retained similar functions

between humans and yeast despite over a billion years of divergence[10,17–20]. Furthermore, the systematic assays involving >1000 human genes cloned in yeast expression vectors revealed properties of genes or genetic modules governing functional conservation[18–22]. The power of systematic screens using toolkits can be estimated by the fact that only ~300 functionally replaceable genes were identified until 2015. Since then, the number of replaceable human genes has doubled [10,16].

"Humanized yeast" is a valuable platform for studying human biological processes in a simplified cellular context [19,23–25]. However, the discovery of highly efficient genome editing tools for humanized yeast studies is not limited to orthologous genes. Genetic toolkits with fully characterized promoters enable systematic screens in yeast of over-expression phenotypes associated with many disease-relevant human genes[20,24,26]. Avenues for research with the Human ORFeome collection include over-expressing human genes in different yeast strains for interesting phenotypes [27,28]. For example, the over-expression of 20 GFP fusion-tagged human genes, toxic to yeast, discovered novel drug targets and repurposing of FDA-approved drugs, expanding the number of available therapeutics for rare and common genetic diseases [29].

1.2 Solutions to increase precision and throughput in cloning.

The impact derived from performing large-scale experiments in yeast provides incentives to continue investing in the next-gen toolkits and creating automated protocols with a need for a compatible new DNA assembly technique. Despite the success of current methods, there is a need for more streamlined and high throughput strategies to obtain clones with precision to enable automated large-scale screens and experiments.

Type IIP restriction enzymes have been historically used for cloning DNA. However, assembling multiple DNA fragments would require distinct enzymes because each type IIP enzyme generates a unique overhang. This strategy is, therefore, unsuitable for the high throughput cloning of many DNA fragments. In contrast, Golden Gate cloning uses type IIS restriction enzymes, recognizing a short sequence in the DNA while creating a double-strand break flanking the binding site [7]. The strategy enables the generation of specifically designed overhangs permitting multi-part modular assemblies. In addition, this technique allows for a scar-less assembly, eliminating the restriction sites from the final product and enabling enrichment. Thus, the precision cloning efficiency increases by cycling the reaction between the digestion and ligation steps, amplifying the correct clones in the mix. Typically a final construct of >9 DNA fragments can be obtained with only a single enzyme digestion, increasing the throughput, complexity and precision in cloning[30] [7]. Golden Gate cloning kits such as MoClo-YTK and DNA-BOT enable automation using colony picker robots and GFP dropout to identify the correct colonies[6,31]. While the fluorescent selection is efficient on a Petri dish where the GFP^+ or GFP^- colonies are well separated, identifying and picking the correct colonies is problematic on tiny spots in a 96 or 384-well format. In addition, as the number of fragments increases, the proportion of incorrectly assembled vectors also increases [7]. This problem worsens if the cloned inserts also harbour the enzyme restriction sites that cannot be eliminated. In these situations, the Golden Gate assembly method leads to many colonies with backbone vectors or incorrectly assembled clones.

Gateway cloning technology uses site-specific recombination to clone DNA, comprising a gene of interest and the destination vector containing a toxic gene cassette "*ccd*B" (disrupts DNA gyrase activity), flanked by specific recombination sites [32]. The recombination exchanges

the toxic gene for the gene of interest in the destination vector. As a result, only the bacteria harbouring the correct clones survive on the selection medium [33]. The strategy increases precision in cloning, with nearly every colony containing the correct clone. In addition, the toxic cassette increases precision by reducing the number of background colonies that fail to grow in a *ccd*B-sensitive *E. coli* strain. However, due to the cost of enzyme kits, performing many plasmid assemblies using Gateway technology can be expensive [34]. Therefore, adapting and combining the Golden Gate and Gateway methodologies may facilitate automated cloning with high accuracy. In addition, precision can be improved by introducing toxic gene selection (like *ccd*B for *E. coli* and *TPK2* for *S. cerevisiae*)[35].

1.3 A new toolkit for functional genomics and synthetic biology in fission yeast

Our laboratory is interested in systematically testing if orthologous genes are functionally equivalent across species [16]. Fission yeast diverged from budding yeast ~400 million years ago, resulting in fission yeast retaining a large proportion of conserved genes with humans as compared to budding yeast[36]. Furthermore, one of the first tests for functional complementation of human genes in distant organisms was performed in fission yeast, discovering a conserved role of a cell cycle protein, *CDC2* [37]. Therefore, fission yeast is a remarkable asset for studying cell and molecular biology relevant to humans[38]. However, since these initial experiments, few humanization assays have been performed in fission yeast [39]. In contrast, many systematic screens were performed, due to the availability of several molecular biology toolkits and strain collections, in the budding yeast and have provided remarkable biological insights. On the other

hand, these tools are limited in fission yeast research and, as a result, hinder our ability to further investigate functional relationships using fission yeast as a eukaryotic model[36,40,41].

Over the past few years, progress has been made towards developing toolkits for fission yeast, such as fully characterized stable integration vectors, Gateway cloning vectors and a CRISPR-Cas9 kit that allows for the introduction of designer auxotrophic strains [4,42,43]. These tools have led to a few large-scale screens in fission yeast that have provided major scientific insights and, as a result, incentivized using fission yeast as a model for systematic studies aided by next-gen toolkits[44–46]. For example, 437 human cDNA clones isolated by microarray analysis of cancerous liver and gastric tissues were studied in fission yeast to determine cellular functions that might be relevant to cancer while developing Gateway-compatible vectors, demonstrating fission yeast as a valuable platform for screening cancer-related human genes [47]. Comparative studies in fission and budding yeast can also be used to investigate other aspects, such as studying human diseases in yeast models[48]. For example, pathogenicity in Huntington's disease is characterized by the expansion of a polyglutamine (polyQ). This molecular mechanism was elucidated by characterizing polyQ toxicity in budding yeast and the lack of toxic phenotypes in fission yeast[49]. Similar studies enabled the discovery of novel and uncharacterized gene functions in yeast and humans[50–52]. These and many more studies emphasize the value of toolkits for fission and budding yeast[53–55]. Most modern toolkits also include next-generation gene editing CRISPR-Cas9 plasmids that are instrumental in systematically deciphering gene function and engineering biology [56].

CRISPR-Cas9 has expanded the ability to perform precise genome editing in many organisms [35]. Modified versions of Cas9, such as deactivated Cas9 (dCas9), allow the

regulation of transcription in budding and fission yeast [57,58]. However, in fission yeast, the expression of Cas9 results in toxicity [59]. Attempts to resolve the toxicity include using codon-optimized Cas9 for fission yeast which were partly successful. However, the efficiency of Cas9-sgRNA-mediated genome editing is still poor compared to budding yeast [60].

While several fission yeast vector collections are available, the cloning strategies are not high throughput [46]. Furthermore, large-scale studies in fission yeast are also hindered by the limited amount of versatile strain collections. For example, the Bioneer collection consists of heterozygous knockouts of essential and nonessential genes in *S. pombe* [61]. However, the collection of essential gene heterozygous knockouts can be purchased only as individual strains and, thus, is expensive for a systematic screen. Therefore, there is a need to introduce a new toolkit to enable large-scale assays in fission yeast, comprising a set of fully characterized promoters, terminators, and modular cloning strategies, enabling automated high throughput assembly of expression vectors with high precision.

1.4 Thesis objectives

Molecular toolkits provide researchers with readily available, efficient strategies to bypass the time-intensive aspects of molecular biology. Additionally, establishing genome foundries requires higher throughput and precision in building complex expression vectors for synthetic biology research. The automated strategies often employ 96 or 384-well formats to generate thousands of vectors compared to single Petri-dish per clone strategies [31,62]. While the current toolkits have solved the efficiency bottlenecks in cloning, they have yet to be adapted for high throughput precision cloning.

For my master's project, I have engineered an automation-compatible toolkit for fission yeast, "Sp-RoboClo," together with "Sc-RoboClo" for budding yeast (developed by Dr. S. Amarnath). RoboClo is a modular toolkit designed for the instruments in genome foundries, permitting a higher rate of precision and efficiency at scale in an automated manner. In the following chapters, I will describe the design and modular assembly compatibility of the vectors and the characterized promoters and codon-optimized Cas9 and dCAS9 I have included in the kit for fission yeast. I will also explain how I used the vectors to functionally characterize human genes in fission yeast.

In Chapter 2, I will describe the design and discuss the high precision and throughput of the toolkit. The toolkit is designed by combining Golden Gate and Gateway technologies to eliminate the need for screening many colonies to obtain a correct clone.

In Chapter 3, I quantified the strength of three fission yeast constitutive promoters and tested 22 budding yeast promoters for their activity in fission yeast. These will allow for a wide range of gene expression in fission yeast. To show the utility of the toolkit, I expressed and showed the correct localization of various human proteins tagged with GFP in fission yeast organelles, demonstrating the vector can assist in studying human gene expression in fission yeast while evaluating the phenotypic consequences of these genes on yeast cells. I also describe the use of the toolkit in investigating human gene complementation assays in fission yeast by introducing the fission yeast or human genes in one of the fission yeast expression vectors under the constitutive promoter.

In Chapter 4, I describe additional genetic engineering tools such as codon-optimized Cas9, dCas9 and sgRNA vectors without toxic effects as observed in previous studies [59]. While our laboratory is interested in using the toolkit for systematic humanization assays in fission

yeast, the toolkit will enable high throughput modular cloning of heterologous gene(s) for both budding and fission yeast.

2. Chapter 2 - RoboClo – an automated modular toolkit for yeasts

The MoClo-YTK EGFP-dropout yields predominantly correct clones in the case of 2- or 3-part cloning (**Figure 2A**). However, the strategy results in a higher background colony count as the number of parts to be assembled increases leading to a decreased true positive rate [6] **(Figure 2B)**. Furthermore, screening for an EGFP$^-$ colony is challenging in a 96-well setup. To eliminate the

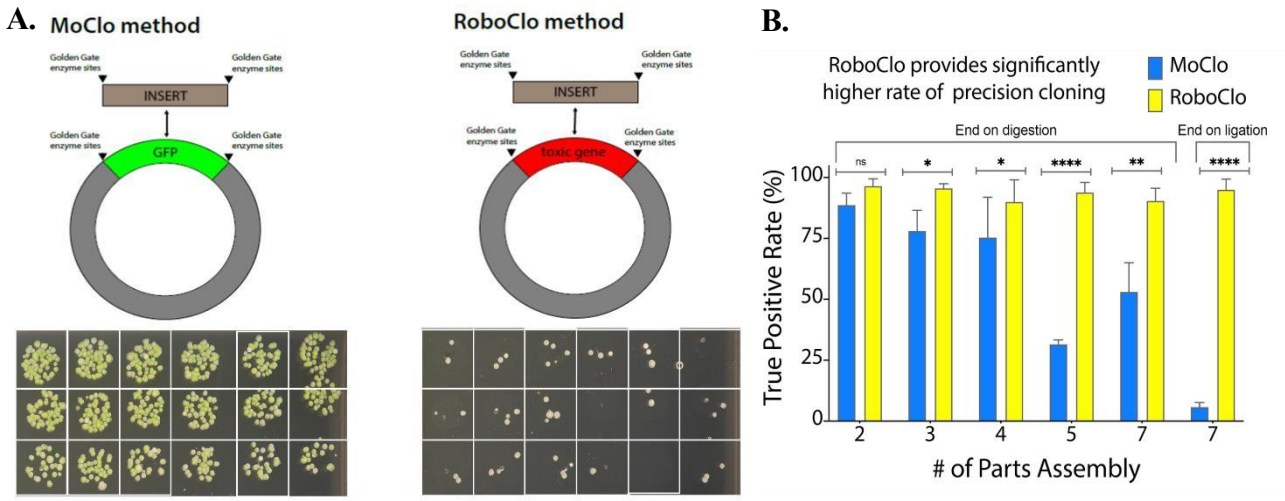

Figure.2 RoboClo enables high precision cloning. ***A****. RoboClo uses a toxic cassette, instead of GFP, dropout to increase cloning efficiency via Golden Gate cloning.* ***B.*** *RoboClo provides a higher rate of precision in cloning. Using GFP dropout and Golden Gate cloning strategy, as the number of parts to be assembled increase, the number of incorrectly assembled clones increases for MoClo. With RoboClo the strategy consistently yields high precision cloning even in the case of strategies where the restriction enzymes sites are retained in the final vector (End on ligation).*

backbone (EGFP$^+$ colonies) and incorrect assemblies, we designed a RoboClo strategy. RoboClo combines the two DNA cloning technologies, Golden Gate and Gateway methods. Using a *ccd*B-dropout (toxic gene selection) to reduce background significantly increases the rate of the correct clones growing on the plate and, as a result, increases the precision in cloning. **(Figure 2A**). The

kit comprises vectors for use in both fission and budding yeast. In the case of Sc-RoboClo (generated by Dr. Smita Amarnath at the Concordia Genome Foundry), many MoClo-YTK plasmids were modified to have *ccd*B selection instead of EGFP-dropout selection[6]. We show that the increased number of assembled fragments results in more incorrectly assembled vectors (**Figure 2B**). Furthermore, we show that the RoboClo strategy increases the rate of true positive clones significantly in the case of more complex cloning (>4 parts) and particularly when the method requires the retention of the restriction enzyme sites (end on ligation). Overall, using a RoboClo backbone and Golden Gate end-on digestion strategy led to a consistently high percentage of true positive clones. The toxic cassette eliminates the incorrectly assembled clones such that only the colonies containing the correct plasmid construct survive. **(Figure 2B)**. Thus, the RoboClo method is adaptable for high throughput automated pipelines in a genome foundry.

The Sp-RoboClo toolkit I built comprises several vectors for fission yeast with type IIS restriction sites creating overhangs compatible with MoClo-YTK plasmids[6]. The Sp-RoboClo plasmids include fully characterized promoters. The basic *E.coli*/*S. pombe* shuttle vectors with *Bsa*I or *Bsm*BI recognition sites flanking EGFP dropout or no dropout enable direct cloning of DNA fragments. In addition, the vectors provide two auxotrophic selections (leucine or uracil) and two antibiotic selection markers (ampicillin or chloramphenicol). The Sp-RoboClo plasmids are also flanked by attR1 and attR2 sites to clone DNA using site-specific recombination

(Gateway strategy) **(Figure 3A)**. The part vectors are *E.coli* vectors containing fission yeast promoters and terminators. **(Figure 3B)**. Type IIS overhangs are identical to the part vectors in the MoClo-YTK, enabling modular assembly of multiple cassettes in fission yeast[6].

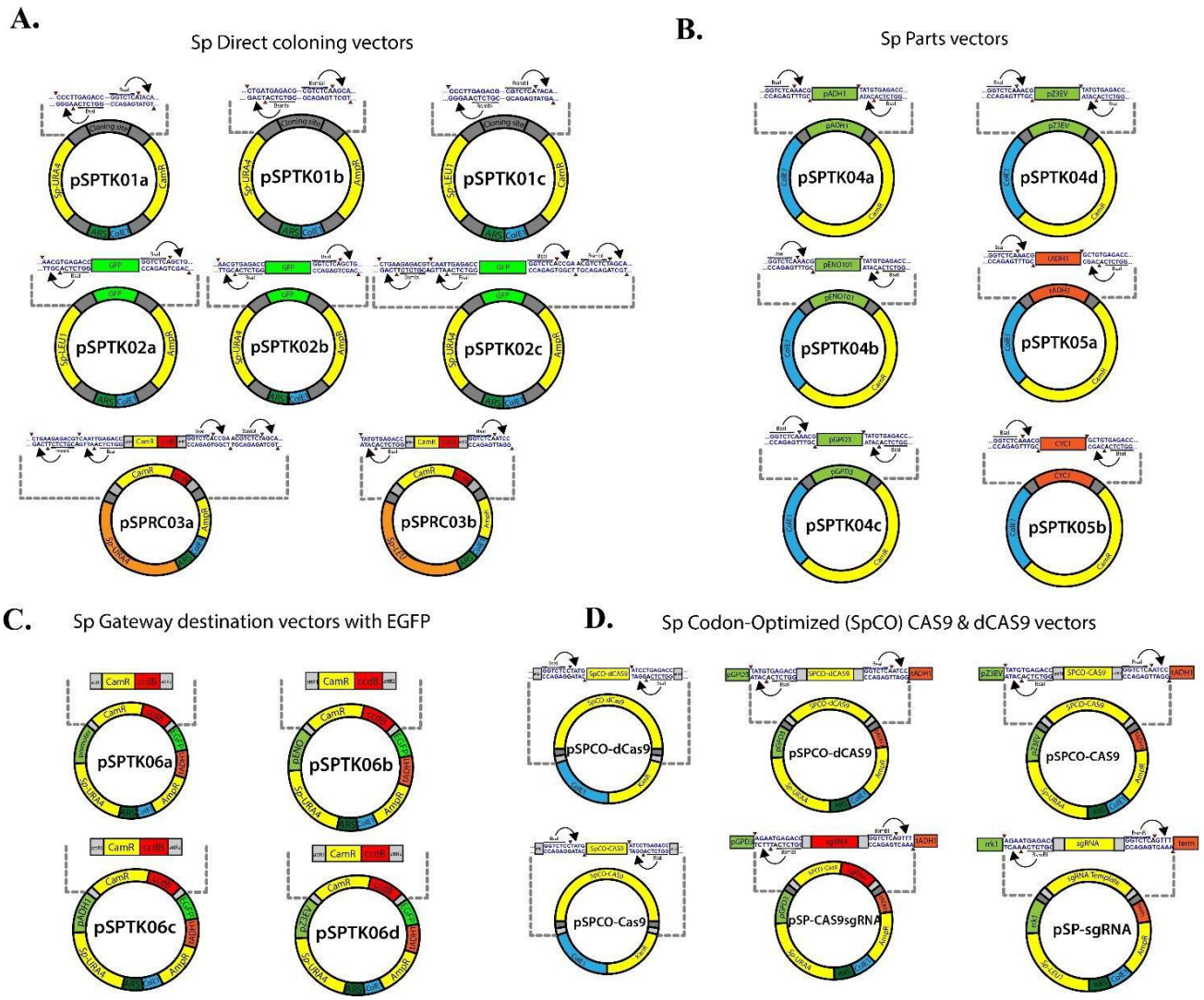

Figure 3. General Overview of toolkit vectors

A. *Direct cloning shuttle vectors harbor one or two distinct Type IIS restriction enzyme sites with various antibiotic and auxotrophic markers. The vectors comprise GFP- (S. pombe toolkit or SPTK) or ccdB- (SPRC or S. pombe RoboClo) dropout cassettes. SPRC vectors are Gateway and Golden Gate compatible.* ***B.*** *Part vectors consist of three constitutive, one inducible promoter and two terminators for fission yeast flanked by compatible Type IIS restriction enzyme sites.* ***C.*** *The Gateway expression vectors for fission yeast comprise different promoters and an in-frame EGFP to create a C-terminal fusion protein with the gene of interest.* ***D.*** *The toolkit provides fission yeast codon optimized Cas9 and dCas9 vectors as well as sgRNA expression cassettes for genome editing in fission yeast.*

The destination vectors comprise SPRC Gateway plasmids that enable C-terminal fusion tagging of genes by LR Gateway cloning **(Figure 3C)**. In addition, these plasmids harbour fission yeast promoter and terminator sequences and allow for uracil auxotrophic selection in fission yeast.

Finally, the kit comprises *S. pombe* codon-optimized (SPCO) CRISPR-Cas9 vectors **(Figure 3D)** with Golden Gate and Gateway cloning strategies, pre-assembled vectors with the Cas9 expression controlled by an Sp*GPD3* promoter and t*ADH1* terminator. Additionally, we designed a new sgRNA expression cassette plasmid with *rrk1* promoter followed by EGFP dropout and Golden Gate enzyme sites to clone in the sgRNA protospacer. The sgRNA contains a scaffold sgRNA sequence followed by a hammerhead ribozyme for appropriate cleavage of the RNA transcript. A new design element introduces a $tRNA^{Arg}$ terminator sequence from the fission yeast for optimal transcription termination. The SPCO-Cas9 or SPCO-dCas9 expressing plasmids can be co-transformed with the sgRNA plasmid and selected on a double-auxotrophic selection (PMG-LEU-URA) medium.

3. Chapter 3 Characterization of constitutive promoters in fission yeast using fluorescent reporter and flow cytometry

Several fission yeast promoters are available, including the most widely used *nmt1* promoter regulated by thiamine. The repressible *nmt1* promoter generates variable expression levels ranging from low to high. The *nmt1* promoter requires growing fission in modified media as yeast extract inactivates the promoter [63,64]. Furthermore, many currently available fission yeast toolkits have limited and, as of yet, quantitatively uncharacterized promoters. Therefore, to expand the promoters for *S. pombe* expression, we characterized the broadly used Sp*ADH1* promoter[63] and introduced two new relatively less-characterized fission yeast promoters, Sp*GPD3* and Sp*ENO101* [65].

To characterize the promoters, we used a RoboClo backbone (pSPTK02b) and generated fission yeast promoter reporters with mRuby (from MoClo-YTK) [6] (**Figure 4**). Flow cytometry showed that *S. pombe pGPD3* is the strongest constitutive promoter, followed by the more commonly used *pADH1*, whereas *pENO101* is a lower-strength constitutive promoter compared to *pGPD3* **(Figure 4A)**. The flow cytometry data for the fission yeast promoters also show population-level effects where some cells are not fluorescing as strongly as others. For example, *pGPD3* is consistent with population-level expression compared to *pADH1* and *pENO101* (**Figure 4B**). The expression of the mRuby reporter was initially characterized using microscopy (**Figure 4C**).

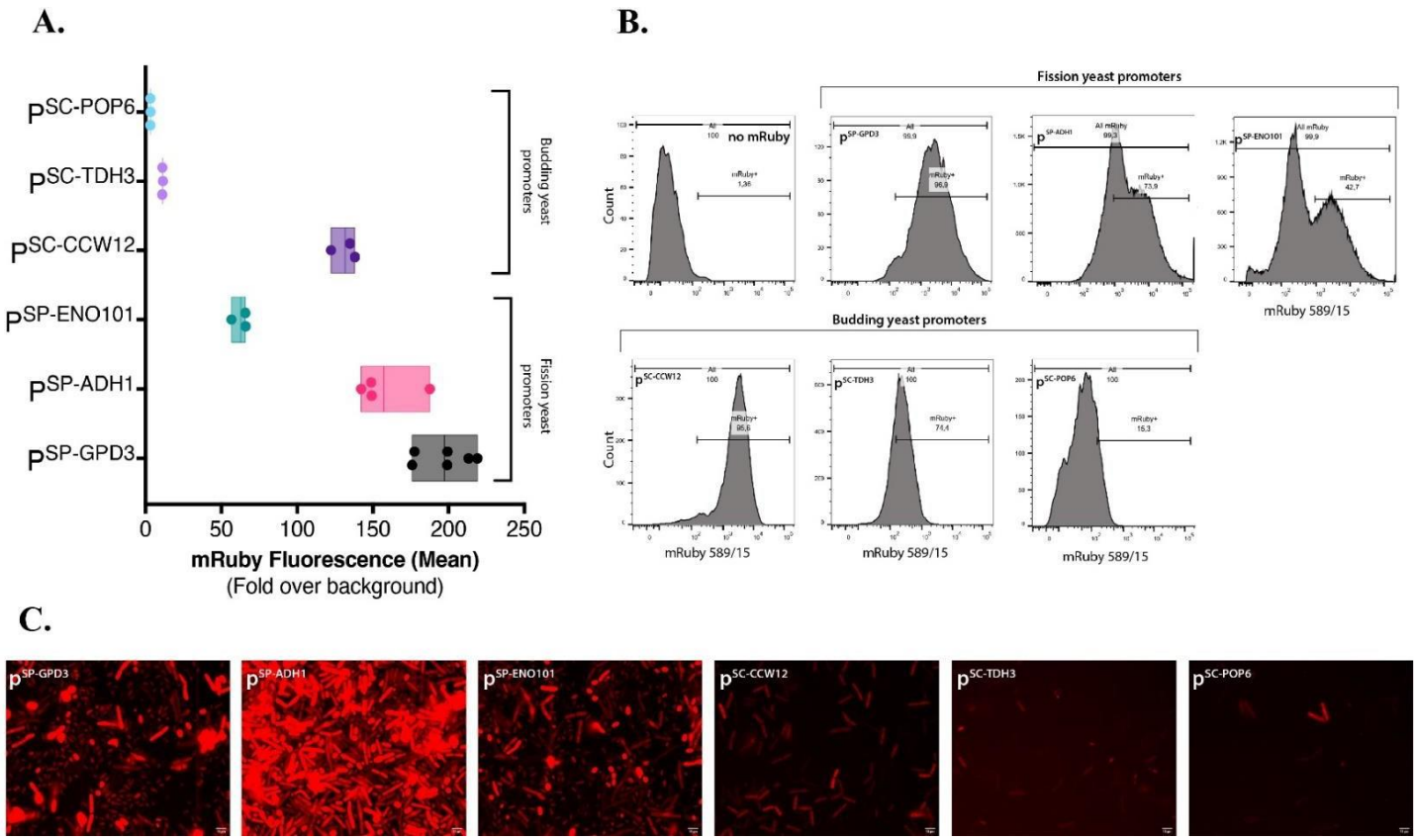

Figure.4 Characterization of fission yeast and budding yeast promoters

Fission yeast promoters and budding yeast promoters from the MoClo kit were assembled into fission yeast expression vectors. ***A****. Median intensity of cell fluorescence for all cells divided by intensity values for negative control to demonstrate expression intensity of each promoter.* ***B****. Fission yeast promoters showed a range of expression in one culture leading to two peaks compared to the budding yeast promoters that showed one level of expression in one culture showing one peak.* ***C****. Fluorescent microscopy using LeicaDM6000B under 50x magnification to confirm fluorescence prior to sending for FACS analysis.*

To further expand the promoters for expression in fission yeast, we generated 22 *S. cerevisiae* promoter-mRuby reporters (from the MoClo-YTK kit [6]) to quantify their transcriptional activity in fission yeast. Only 3 of the 22 budding yeast promoters showed visible fluorescence in fission yeast (**Figure 4C**). Sc-*pTDH3* and Sc-*pCCW12* are known to be strong budding yeast promoters [6]. In fission yeast, Sc-*pCCW12* appeared stronger than the Sc-*pTDH3*

and Sc-*pPOP6* promoters but showed significantly lower expression than the fission yeast promoters **(Figures 4A & C)**. The lack of expression from most budding yeast promoters and significantly lesser orthogonal activity of three strong budding yeast promoters in fission yeast reveals the diverged mechanisms of promoter recognition between the two-yeast species. However, in future, orthogonal promoters could help provide a broader range of promoter expression that can be advantageous in specific experiments.

3.1 Expression of human genes in fission yeast

The EGFP-tagged expression vectors in the RoboClo kit enable tagging a gene of interest with a fluorescent marker. To validate the vectors, we generated four human gene EGFP-tagged expression vectors (obtained from the Human ORFeome collection [27,28]) under the *pADH* constitutive promoter. Human *H3F3* (histone H3.3-nucleus), human *PPOX* (protoporphyrinogen oxidase-mitochondria), *ACTA2* (Actin Alpha 2-cytosol) and *SNCA* (Synuclein Alpha-aggregates upon over-expression), [66]. The EGFP-tagged human gene expression vectors were transformed into wild-type YZY585 fission yeast and visualized by fluorescent microscopy **(Figure 5).**

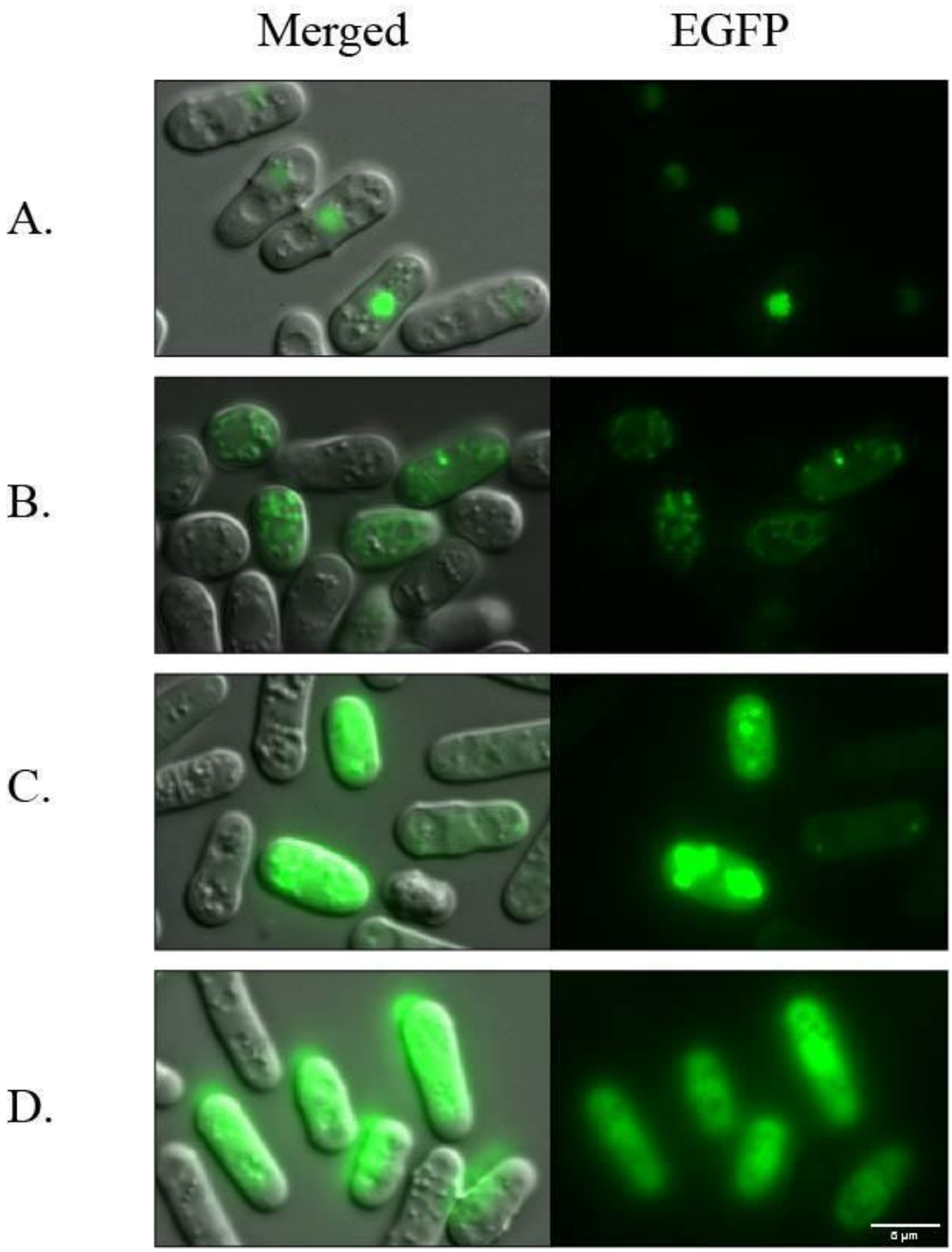

Figure .5 Expression of Human genes in Fission yeast.

Fluorescence microscopy demonstrated the correct localization of human genes in fission yeast. ***A****. H3F3 localization in histones.* ***B****. PPOX localization in mitochondria.* ***C****. SCNA aggregation within the cell.* ***D****. ACTA2 localization in the cytosol.*

We observe strong expression of the human genes in fission yeast and the anticipated localization of the gene products (**Figure 5**). Human histone, *H3F3*, localizes to the nucleus **(Figure 5A)**, human *PPOX* to the fission yeast mitochondria observed as the reticulate pattern of the EGFP expression **(Figure 5B)**, and human *ACAT2* localizes to the cytosol **(Figure 5D).** In contrast, the human *SNCA* appears as aggregates in several individual cells imaged [67] **(Figure 5C)**. The fluorescence microscopy demonstrated that while the human proteins are expressed in fission yeast, there appears to be a population that doesn't show high expression. This anomaly could be attributed to the lack of equal segregation of plasmids between dividing cells [68]. The successful expression and correct localization of the human proteins in fission yeast show that the EGFP-tagged expression vectors are capable of high expression and visualization of heterologous proteins in fission yeast.

3.2 Using RoboClo vectors to test functional complementation in fission yeast.

Humans and fission yeast share several thousand orthologs[36][69]. However, only a handful of studies have tested if the shared human genes are functionally equivalent in fission yeast[39]. Therefore, a systematic screen for testing the functional replaceability of human genes could identify functionally replaceable human genes while revealing properties that govern functional complementation in fission yeast. Sp-RoboClo vectors enable the expression of human genes (using the Human ORFeome collection) under select promoters using high-throughput automated workflows[27,28].

To test functional complementation, we used the Bioneer heterozygous diploid fission yeast strains with one allele of the gene replaced by a *kanMX* cassette [61]. Given that diploid fission yeast tends to sporulate spontaneously, the Bioneer strains carry an *h+/h+* mating-type

locus genotype (compared to *h+/h-* in the wild type), maintaining them as stable diploids [70]. Fission yeast *h+* cells produce the M factor, while *h-* cells produce the P factor. For a cell to perform meiosis and sporulate, both M and P factors must be expressed[71]. The strains also harbour two distinct *Ade6* alleles, *Ade6-M210* and *Ade6-M216*, on separate homologous chromosomes with different point mutations leading to adenine auxotrophy in a haploid state. However, in a diploid state, due to inter-allelic complementation, the strains are adenine prototrophs [61] Thus, the strategy enables a simple readout of the haploid or diploid status of fission yeast cells.

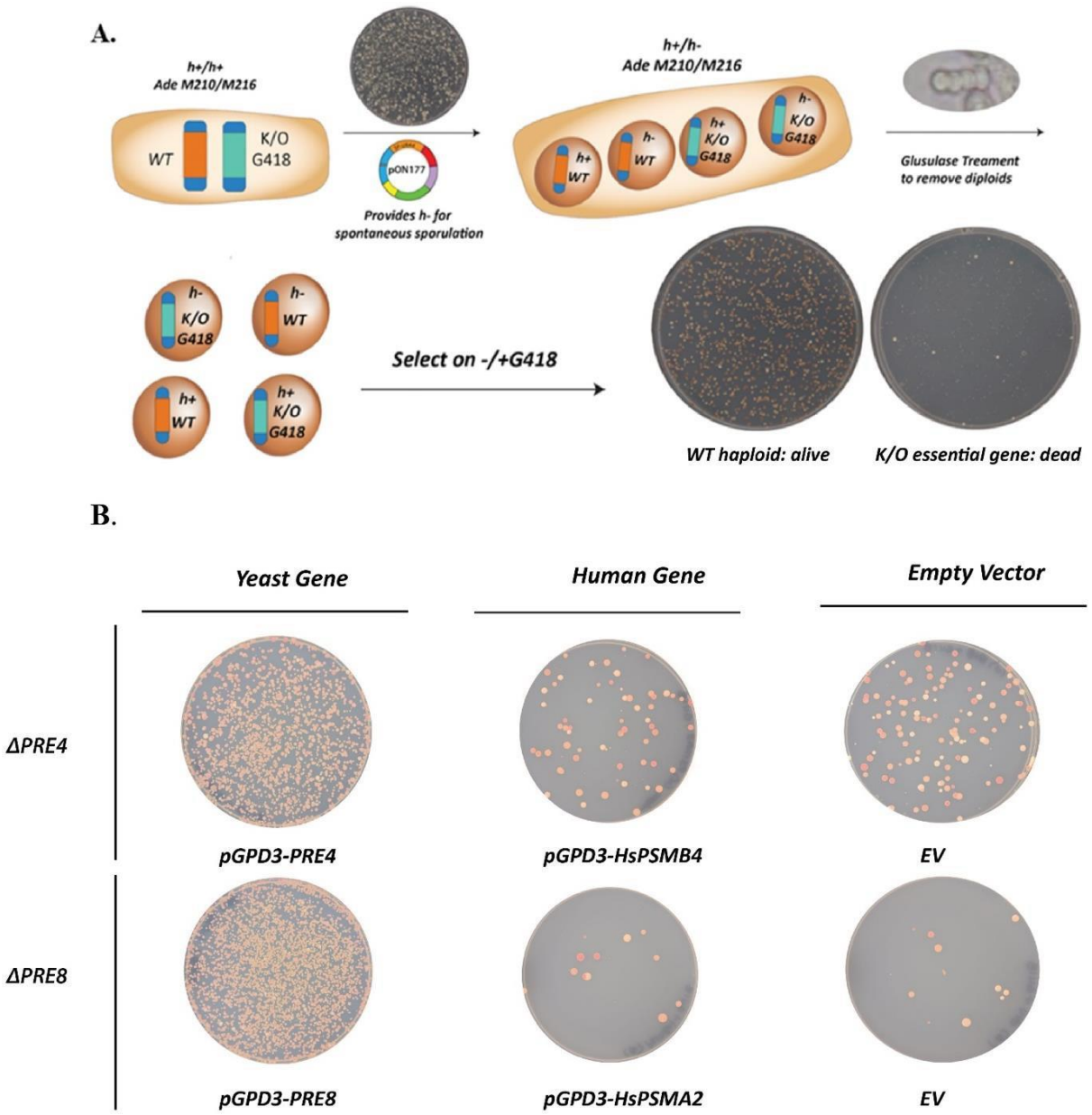

Figure 6. Human gene functional complementation using Bioneer heterozygous diploid knockout strains.

A. *Strategy to test human gene complementation in fission yeast using Bioneer strains. Sporulation is induced by expressing h- factor on plasmid. Random spore analysis is performed with the use of glusulase. Spore mix is plated on selection medium to observe complementation.* ***B.*** *Human or yeast gene with Sp-GPD3 promoter expression vectors transformed into the Bioneer strains prior to sporulation. Empty vector harboring no human or yeast genes show very few red colonies (right panel). Expression of yeast (pre4) and yeast (pre8) in the corresponding Bioneer strains show functional complementation (left panel). However, human gene Psmb4 and Psma2 expression in the corresponding Bioneer strains shows few red colonies similar to empty vector suggesting no functional complementation.*

The Bioneer diploid strains are adenine prototrophs, expressing both *Ade6* alleles, and the colonies appear white [72]. Upon sporulation, the haploid strains receive a single mutant non-functional allele of the *Ade6* gene and are adenine auxotrophs, appearing as red colonies **(Figure 6A)**.

Sporulation is induced by transforming the plasmid expressing the *h-* factor (pON177) in the heterozygous knockout diploid Bioneer strains. The selection of spores on selective media with or without G418 enables the test for the gene's essentiality. We tested for functional complementation using essential proteasome subunit heterozygous knockout strains (*h+, orf Δ:: kanMX4/ORF ade6-M210/ h+, ade6-M216 ura4D-18/ura4-D18 leu1-32/leu1-32*) and heterologous expression of either the fission yeast or the human versions of the genes.

After inducing sporulation, glusulase treatment kills most diploid vegetative cells, allowing the haploid spore population to survive. For the random spore analysis, the spore mix is plated on medium with or without G418; this selection provides for testing of functional complementation. Without G418, the haploids carrying the wild-type gene will grow as red colonies. However, in the presence of G418, neither the wild-type nor the knockout allele carrying haploid spores will grow as the haploid spore with the wild-type allele lacks the selection marker, and the one with the knockout allele is inviable. If the fission yeast or human gene expression rescues the knockout of the essential gene, the red haploid colonies should grow in the presence of G418. We show that the heterozygous diploid strains harbouring the corresponding fission yeast gene on plasmids functionally complement, as indicated by the growth of many red colonies on media containing G418 **(Figure 6B, left panel)**. However, the human versions of these genes fail to complement the knockout of the corresponding yeast genes, as the number of

surviving red colonies was significantly lower relative to the positive control (fission yeast genes on a plasmid) **(Figure 6B, middle panel)** and similar to the empty vector transformations **(Figure 6B, right panel)**.

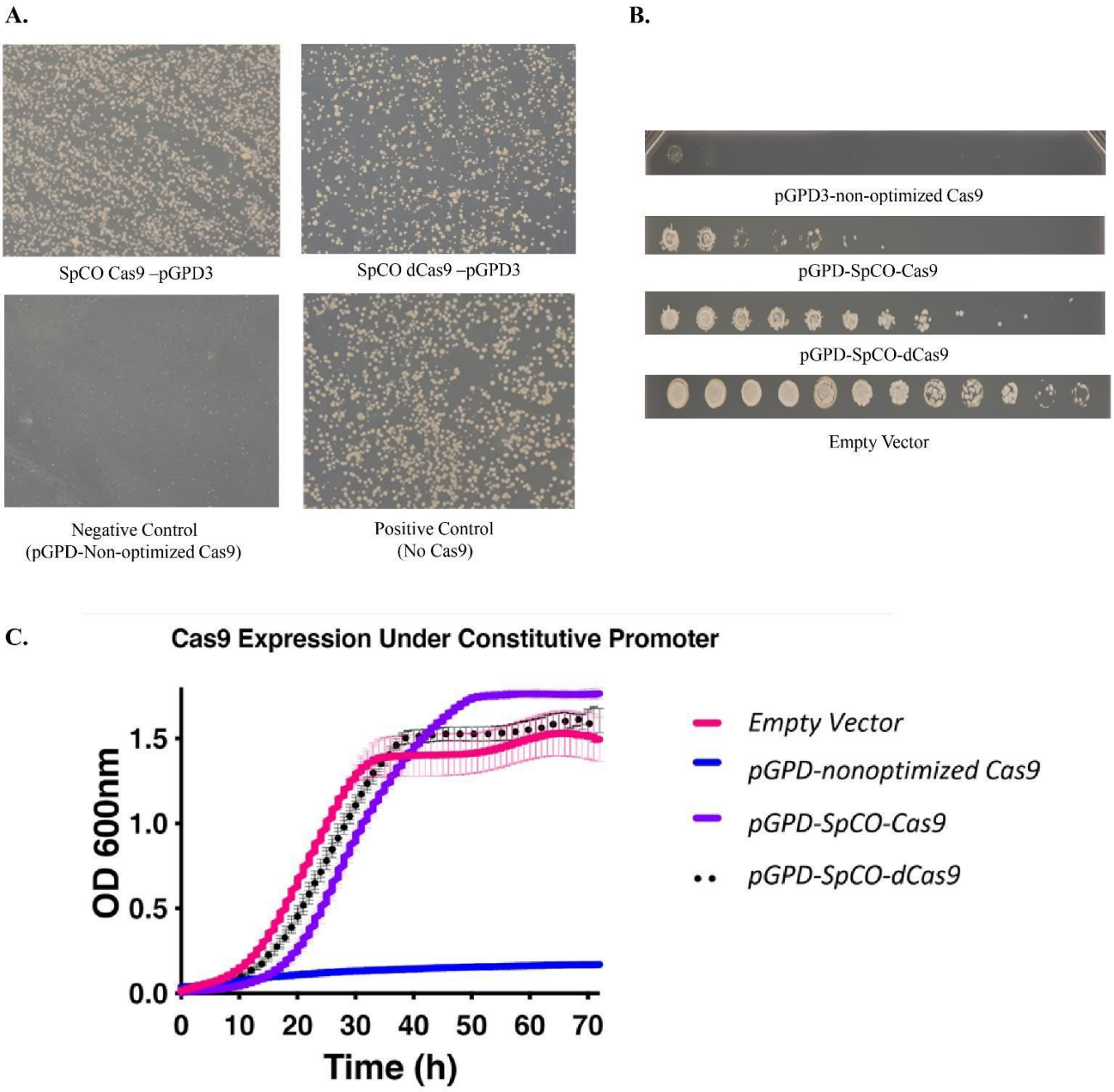

Figure. 7 Codon Optimization relieves toxic phenotypes in fission yeast.

A. *Codon optimized SPCO-Cas9 and SPCO-dCas9 plated on Petri dishes under a constitutive promoter along with a positive control (no Cas9), and a negative control (a vector expressing toxic Cas9).* ***B.*** *Restoration of colony phenotype by codon optimization verified with a diluted spot assay using 1/10 serial dilutions.* ***C.*** *Growth curves were performed to confirm that codon optimization improved cell viability.*

4. Chapter 4 Using Cas9 Codon-Optimized for expression in fission yeast

Previous studies have shown that the expression of a human codon-optimized Cas9 in fission yeast causes toxicity. Fission yeast cells harbouring the Cas9 expression plasmid grow poorly and can mutate the Cas9 gene, resulting in inefficient double-stranded breaks (DSBs)[59]. We hypothesized the following reasons for the Cas9-mediated toxicity in fission yeast: (1) a high number of off-target effects, (2) over-expression of the gene, or (3) incompatible codon use of the human codon-optimized Cas9. The first two hypotheses could be ruled out, given that the use of Cas9 across diverse hosts has shown no significant off-target effects and overexpression toxicity[73]. However, due to codon bias, overexpressing genes with non-optimal codons can cause growth defects and inaccuracies in translation which could lead to toxic phenotypes [74]. Therefore, we designed fission yeast codon-optimized Cas9 and dCas9 genes (using the codon optimization tool offered by Integrated DNA Technologies) to relieve toxicity while improving protein expression.

The expression of the codon-optimized SPCO-Cas9 and SPCO-dCas9 under a constitutive promoter in wild-type fission yeast resulted in normal-sized colonies similar to the empty vector control transformed cells**.** In contrast, the expression of the non-optimized Cas9 gene shows significant growth defects observed as small colonies **(Figure 7 A&B)**. The cultures were spotted as serial dilutions and further characterized using quantitative growth assays, confirming the suppression of the toxic phenotype upon SPCO-Cas9 and SPCO-dCas9 expression **(Figure 7C)**.

We engineered a new sgRNA expression plasmid to complement the codon-optimized SPCO-Cas9 vector. The sgRNA requires precisely defined 5′ and 3′ ends to produce a functional Cas9/sgRNA ribonucleoprotein [75]. We used the previously characterized fission yeast *rrk1* promoter to drive the expression of the sgRNA [59], followed by a scaffold RNA and a hammerhead ribozyme to precisely determine the 3' end of the sgRNA [76,77]. Furthermore, a transcriptional terminator from the native fission yeast $tRNA^{Arg}$ is added to improve the optimal termination of the sgRNA transcript [78]. To test the efficiency of sgRNA-SpCOCas9 expression, we designed sgRNA targeting the *S. pombe Ade6* gene. The complex of SPCO-Cas9-$sgRNA^{Ade6}$ should generate a DSB within the *Ade6* locus. Successful DSB should lead to lethality. In the absence of any external repair template, the DSBR via error-prone non-homologous end joining (NHEJ) pathway results in indels, frame-shift or nonsense mutations, mimicking a knockout phenotype. *Ade6* gene knockout results in the accumulation of byproducts in the pathway within the cell, resulting in a red colour colony phenotype [44]. Thus, the number of red colonies can determine a successful ON-target Cas9-$sgRNA^{Ade6}$ DSB efficiency (**Figure 8D**).

The negative vector controls consisting of the SpCO-Cas9 and SpCO-dCAS9 with no sgRNA show many white-coloured colonies, suggesting no DSB generation **(Figure 8A & C).**

However, the expression of SPCO-dCas9-sgRNA^{ade6} shows several red colonies, demonstrating a transcriptional disruption of the adenine pathway **(Figure 8B)**. Furthermore, the expression of a SPCO-Cas9-sgRNA^{Ade6} **(Figure 8D)** lethal phenotype suggests ON-target activity, and surviving colonies appear red, indicating mutations at the *Ade6* locus (**Figure 8E**). Colony PCR and Sanger sequencing of the *Ade6* locus for one of the red colonies revealed a frame-shift mutation within the sgRNA target region **(Figure 8E).** We tested the co-expression of the Cas9 and sgRNA cassettes in a single vector for fission yeast could improve efficiency. However, all the colonies on the plate show an off-white phenotype. This plasmid construction strategy will require further optimization to eliminate assembly challenges. However, the co-expressing Cas9-sgRNA plasmid is included in the kit.

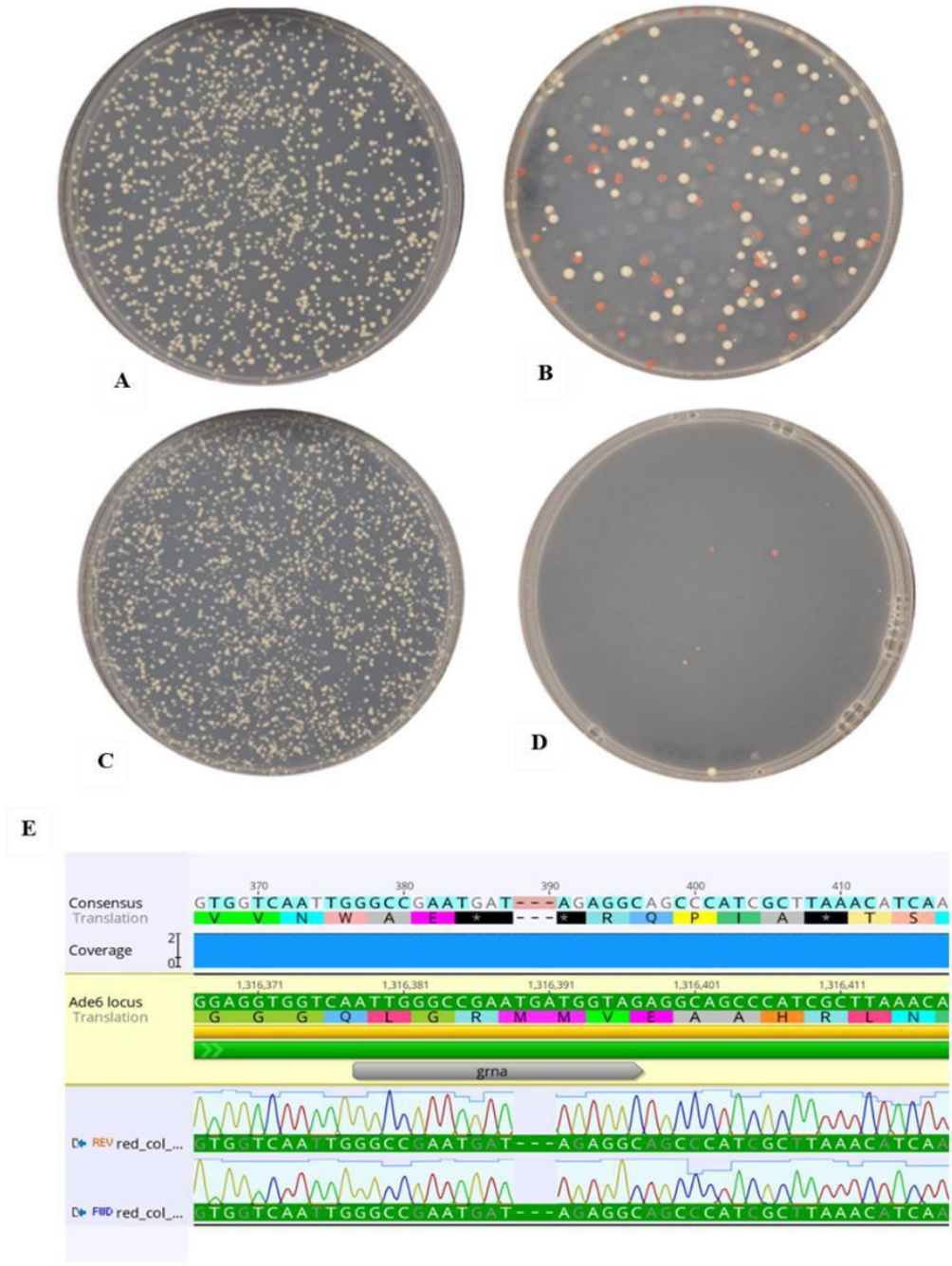

Figure.8 Codon optimized SPCO-Cas9 and SPCO-dCas9 targeting the Ade6 gene in wild-type fission yeast.

*A wild-type fission yeast strain was transformed with vector carrying **A.** SPCO-Cas9 and **C**, SPCO-dCas9 plated on PMG-URA. Colonies are viable and grow to normal size as expected. Plasmid with sgRNA targeting the Ade6 locus transformed into strain with **B.** SPCO-Cas9 plasmid and **D**.SPCO- dCas9 plasmid resulting in red colonies. **E**. Colony PCR on red colony to verify sgRNA target site.*

5. Chapter 5 - Conclusion

For my master's project, I developed a molecular cloning toolkit offering high-precision cloning for fission and budding yeast. The RoboClo toolkit combines Golden Gate and Gateway technologies, eliminating the need to screen multiple colonies to obtain correct clones. The toolkit opens up avenues to perform modular cloning of many genes at scale for budding and fission yeast.

First, I demonstrated that toxic gene dropout selection (*ccd*B*)* increases the rate of precision cloning for complex DNA fragment assemblies. Next, by characterizing several fission yeast and 22 budding yeast promoters in *S. pombe*, I characterized six constitutive expressing promoters, three native to fission yeast and three orthogonal promoters from budding yeast, with variable levels of expression[6]. Furthermore, I show that the expression of fission yeast codon-optimized SPCO-Cas9 and SPCO-dCas9 (catalytically dead) reduces the toxicity caused by the expression of human codon-optimized Cas9 in *S. pombe*. These SPCO-Cas9/dCas9 vectors can be used for high-efficiency genome editing in fission yeast.

Moreover, the toolkit comprises EGFP vectors that enable the expression of fusion proteins tagged with *GFP* in *S.pombe*. Using the EGFP vectors, I show human gene expression and optimal localization of the gene products, demonstrating the conservation of localization signals in the fission yeast. These expression systems enable the study of many human genes and their variants in fission yeast. Furthermore, the system allows testing of human gene expression phenotypes like toxicity in fission yeast and their comparative phenotypes in budding yeast. For example, the expression of SNCA (alpha-synuclein) is toxic in budding yeast but not fission yeast, thus allowing the molecular characterization of human gene expression phenotypes in diverse species [67].

Finally, I used RoboClo vectors to perform complementation assays in heterozygous diploid knockout fission yeast strains (from Bioneer). By introducing fission yeast genes on plasmids, I demonstrated the complementation of the knockout of an essential gene in *S.pombe*. Given our laboratory's interest in deciphering orthology-function relations using systematic functional complementation assays and significant conservation between humans and fission yeast, these toolkits and assays provide a platform for systematic functional complementation of human genes in fission yeast.

While successful, these assays are not compatible with a high throughput screen. Introducing an additional vector for sporulation and the glusulase treatment adds steps that may be difficult to scale. In addition, an entire Bioneer strain collection will be required to systematically screen human genes for functional complementation, which will become a costly endeavour (~$200 per strain). We propose an alternative method using the optimized SPCO-Cas9 to target yeast genes and introduce the orthologous human gene on another RoboClo vector to assay for replaceability. Alternatively, we can use SPCO-Cas9 and SPCO-dCas9 to knockout or transcriptionally repress essential fission yeast genes and screen for human gene complementation. Unlike the previously described Bioneer method, we can use the Cas9 plasmids to target essential genes in fission yeast at a more high-throughput method. The Cas9 will create a DSB which will be repaired by NHEJ, leading to deleterious mutations and cell death. However, by co-transforming the human orthologue on the fission yeast plasmid, the cells harbouring the human gene that complements the function of the knockout allele will survive. This could be a more feasible approach that can be scaled up to assaying all the essential genes using the automated platforms available in the genome foundry and can be performed using the Roboclo toolkit for fission yeast.

Therefore, RoboClo provides the ability to perform small-scale experiments with the existing tools for fission yeast and yet can also be used to scale up the same experiment for systematic analysis. It can also enable automated high throughput assembly with precision using instruments found in genome foundries.

6. Chapter 6 - Materials and Methods

6.1 Golden Gate Assembly Protocol:

Each Golden Gate reaction tube was prepared as follows: 20fmol of DNA backbone vector and 40fmol of DNA insert, 1 μL T7 ligase (3x10^6 units/ml); (NEB; M0318S), 1μL 100mM ATP (ThermoFisher; R0441), 1μL of 10 U/μL restriction enzyme, 1 μL of 10X enzyme buffer and water to make a final volume of 10μL. Each reaction mixture was incubated on a thermocycler with the following program: 30 cycles of digestion and ligation (37ºC for 1 min, 16ºC for 1 min) followed by a final digestion step (end-on-digestion at 37 ºC for 15 min) or final ligation step (end-on-ligation at 16 ºC for 30 min) and a heat inactivation step (85 ºC for 15min).

6.2 Gateway Assembly Protocol:

The Gateway reaction tube was prepared as follows: 150 ng of DNA insert, 150 ng of destination or entry vector, 1X TE buffer (pH 8.0) to a final volume of 8 μL. The reaction was completed with 1 μL of BP or LR clonase (Invitrogen; 11791020, 11789100). The reaction mixture was incubated at room temperature overnight. The next day 1μL of Proteinase K (Invitrogen; 11791020, 11789100) was added to the reaction mixture to stop enzyme activity. The reaction was transformed in *ccd*B sensitive DH5α *E.coli* competent cells and plated on LB agar with antibiotic selection.

6.3 High-precision cloning assay using SC-RoboClo

To analyze cloning precision, DNA fragments were assembled using MoClo-GFP (*CamR*) and RFP (*AmpR*) backbone vectors, followed by cycling the Golden Gate reaction to end on digestion. The selection of GFP+ and Ampicillin resistant colonies suggests correct assembly. In the case of

Sc-RoboClo vectors with a *ccd*B dropout, the plasmids extracted from the surviving colonies were tested for correct assemblies using restriction enzyme digestion.

6.4 *E. coli* Transformation and Plasmid prep

50ng of DNA was added to 50 µL of *E.coli* competent cells. The reaction was incubated on ice for 30 min. The transformation mix was then placed in a 42ºC water bath for 30 seconds and immediately incubated on ice for 5 min. A volume of 950 µL of room temperature Luria Broth (LB) media was added to the reaction mix and incubated at 37 ºC with shaking for 45min at 200rpm. The reaction was spun at 8000 rpm for 3 min, resuspended in 300 µL of water and plated on antibiotic-containing LB plates as per high-efficiency NEB® 5-alpha Competent *E. coli* protocol (cat: C2987H). The plates were incubated at 37 ºC for 18-24 hours. DNA was isolated following instructions for the Qiagen miniprep kit (cat: 27106X4) or midiprep kit (cat: 12943).

6.5 *S. pombe* Competent Cell Preparation and Transformation:

An initial culture from a glycerol stock was incubated in liquid culture at 30ºC with shaking at 250 rpm overnight. The culture was then diluted to an O.D. of 0.3 measured at 595 nm in a final volume of 50 ml media. At O.D. 0.5 (595nm), the culture was centrifuged for 5 min at 3500 rpm. The pellet was suspended in 50 ml of dH20 water, centrifuged for 5 min at 2500 rpm, and the pellet is suspended in 1ml of 0.1 M Lithium Acetate/TE buffer solution and 20 µL of freshly boiled 10 mg/ml single strand salmon sperm DNA (Invitrogen;15632011V). Then 100 µL of cells were taken for each transformation reaction, and 1 µg of plasmid DNA was added with incubation at room temperature for 10 min. Subsequently, 260µL of PLATE solution (40% PEG,

0.1M LiAc, 10xTE) was added and incubated for 60 min at 30ºC with shaking at 250 rpm. DMSO (43µL) was then added to the reaction with heat shock for 5 min at 42ºC and centrifugation for 5 min. at 3500 rpm. The pellet was washed with water and then centrifuged for 5 min. at 3500 rpm. The resulting pellet was suspended in 500 µL water and plated on the selection medium. For G418 selection, strains were incubated for 1 hour in YES medium before plating[44]. Transformations were also performed using the Zymogen 930 frozen EZ yeast transformation kit. (Cedarlane; T2001).

6.6 Sporulation of diploid strains and selection of haploid strains:

Diploid strains were sporulated in a solution of potassium acetate (10%) and zinc acetate (0.5%) for 3-5 days. Sporulation efficiency was verified by microscope. For random spore analysis, 20 µL of spore solution was treated with 5 µL of glusulase enzyme (Perkin Elmer cat: NEE154001EA). The Glusulase treated mixture was incubated overnight at room temperature. The spore solution was then diluted 10-fold with water and plated on a selection medium to grow the haploid cells.

6.7 Flow cytometry Analysis of fluorescence expression in yeast

Cells expressing mRuby were inoculated in an overnight culture and sent for Fluorescence-activated cell sorting (FACS) on the Bio-Rad ZE5 (Yeti) cell analyser at IRIC. The samples were submitted in triplicates. To compare expression levels of the functional *S.cerevisiae* promoters to the *S. pombe* promoters, the total mean fluorescence readout per promoter was divided by the fluorescence of the negative control and plotted.

6.8 Strains and Growth Media:

The *S. pombe* strain used to characterize the promoters and vectors in this kit was YZY585 *(h+, ura4-D18, leu1-Δ0),* obtained from Dr. Jeff Boeke. The Bioneer strains used for complementation were BD_D4821 and BD_D0303 (*h+, orf Δ:: kanMX4/ORF ade6-M210/ h+, ade6-M216 ura4D-18/ura4-D18 leu1-32/leu1-32*) . Standard YES complete and PMG minimal media from Sunrise Sciences were supplemented with 0.255 mg of the amino acids histidine, adenine, leucine, lysine and uracil combined with a final agar concentration of 2% (Sigma Aldrich cat: A5306-250G). When necessary, liquid G418 (Thermo Fisher; 10131035) was diluted to the final concentration of 200μg/ml.

The *E.coli* competent cells were made following the rubidium chloride protocol [79]. When cloning *ccdB-resistant* vectors, transformations were performed in One Shot™ *ccd*B Survival™ 2 $T1^R$ Competent Cells (ThermoFisher;A10460).

E.coli competent cells and cultures were grown in LB media supplemented with ampicillin (100 μg/ml), chloramphenicol (35 μg/ml), or kanamycin (50 μg/ml). Agar (Sigma Aldrich cat: A5306-250G) was added to a final concentration of 2% for the preparation of solid media.

6.9 Strategy for Construction of Sp-RoboClo

Direct Cloning Vectors

The first vector, pSPTK01a, was built by restriction digestion with *Bsm*BI and gel extraction of the origin of replication (*ori1*) and chloramphenicol selective markers for *E.coli* from pytK001 as one fragment. The origin of replication for fission yeast was PCR amplified from vector pMZ374 with *Bsm*BI overhangs. The *URA4* gene was ordered as a G-block from IDT to remove internal restriction sites and add correct overhangs for *Bsm*B1 Golden Gate assembly and two *Bsa*I recognition sites in the terminator for cloning. The PCR fragments were gel extracted using the gel extraction kit (Qiagen cat: ID:28706X4), and the vector was assembled using enzyme *Bsm*B1 and cycling Golden Gate cloning to end-on-digestion. To construct pSPTK01b, the origin of replication and ampicillin selection marker was digested with *Bsa*I and gel extracted from pytK095. The origin of replication for fission yeast was PCR amplified from vector PMZ374 with *Bsa*I overhangs. The *URA4* gene ordered as a G-block from IDT was PCR amplified with overhangs for *Bsa*I Golden Gate assembly and two *Bsm*BI recognition sites in the terminator for cloning. The DNA fragments were gel extracted and assembled by Golden Gate at the end-on-digestion. Vector pSPTK01c was constructed similarly to vector pSPTK01b, except that a *LEU1* gene (instead of the *URA4)* was PCR amplified from the fission yeast genomic DNA with *Bsm*BI cut sites in the terminator for cloning.

EGFP Direct Cloning Vectors

To create pSPTK02a with an EGFP dropout, the EGFP was PCR amplified from pYTK047 with *Bsa*I and *Bsm*BI cloning sites. The EGFP fragment was inserted into pSPTK01b by *Bsm*BI Golden Gate end-on-ligation to retain the recognition site for *Bsa*I and *Bsm*BI for

cloning into pSPTK02a. To assemble pSPTK02b and pSPTK02c, an EGFP fragment flanked by *Bsa*I cut sites were inserted into pSPTK01b and pSPTK01c, respectively, using Golden Gate end-on-digestion. The overhangs for pSPTK02b were created to be compatible with the MoClo-YTK kit for generating a transcriptional unit using promoter or terminator inserts.

Generation of *ccd*B Direct Cloning Vectors

The *ccd*B vector pSPRC03a was created by PCR amplifying the *ccd*B and chloramphenicol cassettes as a PCR fragment with *attB* sites and *Bsa*I sites from pAG416GPD-*ccd*B. Next, this fragment was added to the backbone vector pSPTK02a by cycling Golden Gate cloning to end-on-ligation due to the internal *Bsa*I cut sites in the *ccd*B cassette. This strategy provided the *Bsa*I and *Bsm*BI sites for future cloning. For pSPRC03b, the *ccd*B cassette was amplified with *Bsa*I sites and inserted with pSPTK04c(*pGPD3)* and pSPTK05a (*tADH1*) into pSPTK02c with Golden Gate end-on-ligation. For pSPRC07a,b,c and d, the *ccd*B-*EGFP* cassette was PCR amplified from PAG416GAL-*ccd*B-EGFP to create the EGFP-tagged expression vectors. Finally, the *ccd*B-EGFP fragment with *Bsa*I sites was inserted into backbone vector pSPTK02b with the promoters from pSPTK05a,b,c,d and terminator found in pSPTK06a by Golden Gate end-on-digestion. The *ccd*B insert in these constructs was sequence-verified to ensure no mutations were introduced while assembling.

Part Cloning Vectors

The part vectors pSPTK05a,b,c,d and pSPTK06a,b were created by PCR amplifying *GPD3, ENO101*, *ADH1* and *CYC1* from a genomic prep of wild-type fission yeast YZY585. These fragments were gel extracted and assembled with pYTK001 using Golden Gate end-on

digestion cloning. Except for *ADH*1, end-on-ligation due to internal *Bsm*BI restriction sites. *TADH1* was PCR amplified from the vector pBMod-Tadh-Kan(de), with the internal *Bsm*BI sites removed. *Z3EV* was obtained from PCR amplification of the vector PFS462.

6.10 Strategy for constructing 22 *S. cerevisiae* promoters in fission yeast

Twenty-two *S. cerevisiae* promoter part vectors and the mRuby part vector pytK034 were obtained from MoClo-YTK. These promoters were cloned into pSPTK02b with pSPTK05a carrying *TADH1* from Sp-RoboClo for a total of twenty-two Golden Gate end-on-digestion reactions. MμLtiple GFP- colonies per reaction were isolated and verified by the robotics available in the genome foundry at Concordia University. Correct clones were confirmed by restriction digestion. The three constitutive fission yeast promoters were cloned in pSPTK02b with mRuby. The clones were transformed into YZY585 wild-type fission yeast and plated on PMG-URA. The cells were screened using the Leica DMI6000B inverted epifluorescence microscope (refer to 6.11).

6.11 Constructing plasmids for expression of human genes in fission yeast

Human gene cDNAs were obtained from the Human ORFeome collection V. 7.1[27,28]. The genes *ACTA2, PPOX, H3F3*, and *SNCA* in LR-compatible PDONR223 were prepared from glycerol stocks individually. These vectors were LR cloned into pSPRC06c carrying pADH1 promoter and tADH1 terminator with an EGFP fusion protein tag. The clones were then transformed into wild-type fission yeast YZY585 and plated on PMG-URA. Cells were visualized on the Leica DM6000B epifluorescent microscope (refer to 6.11).

6.12 Microscope analysis of expression using fluorescent markers in fission yeast

Microscope analysis of EGFP-tagged human genes was prepared by inoculating colonies in water and observing on the Leica DM6000B epifluorescent microscope at 100x oil immersion with 10x magnification. Microscope analysis of expression of the 22 *S. cerevisiae* promoters in *S. pombe* was prepared by inoculating colonies in water and pipetted into a 96-well plate with a coverslip bottom (Ibidi;89626) for microscopy. The cells were screened using the Leica DMI6000B inverted epifluorescence microscope, 63x oil immersion with 10x magnification. All microscope analysis was performed at the Centre for Microscopy and Cellular Imaging at Concordia University. Images were edited using ImageJ software.

6.13 Testing for gene essentiality in Bioneer Strains

Human gene cDNAs were obtained from the Human ORFeome collection V. 7.1[27,28]. The plasmids carrying the genes human *Psmb4* and *Psma2* in LR-compatible vector pDONR223 were isolated from glycerol stocks. The yeast genes, *Pre4* and *Pre8*, were PCR amplified from fission yeast genomic DNA with *attB* compatible sites and BP cloned into PDONR221 to make them LR-compatible plasmids. The yeast and human genes were then LR cloned into pSPRC03b.

The pON177 plasmid, which carries the *h-* factor (obtained from Dr. Olaf Nielson), was transformed into the Bioneer strains and plated on PMG-URA+G418. These strains were then transformed with the human and yeast genes and plated on PMG-URA-LEU+G418 yielding white diploid colonies. These colonies were then sporulated and plated on PMG-LEU-URA+/-G418.

6.14 Strategy for construction of SPCO-Cas9 and SPCO-dCas9 vectors

SPCO-Cas9 and SPCO-dCas9 genes were codon-optimized by inserting the gene of interest in the IDT codon optimization tool. By selecting the target species, the program rearranges the sequence based on the frequencies of the preferred codon usage. It removes codons with less than 10% frequency and normalizes the remaining frequencies to 100%. In addition, it simplifies the sequence submitted to remove downstream effects such as hairpins, repeats and high GC content (https://www.idtdna.com/pages/tools/codon-optimization-tool). The genes were designed with *Bsa*I and *attB* sites for Gateway and Golden Gate assembly. SPCO-Cas9, SPCO-dCas9 (designed using IDT) and non-codon optimized Cas9 from pytK036 were assembled into pSPTK02b under the *pGPD*3, *pZ3EV* and *tADH*1 part vectors by Golden Gate end-on-digestion to make pSPCO-Cas9, dCas9. The Cas9 from vector pYTK036 was also assembled into pSPTK02b to compare toxic expression with the codon-optimized genes.

The sgRNA scaffold was designed as a gBlock (IDT) with a GFP dropout where the sgRNA-target sequence will be inserted by Golden Gate. The sgRNA scaffold was assembled into pSPTK02c to make pSP-sgRNA. Similarly, a plasmid with *URA4* cassette was generated by Golden Gate cloning of the sgRNA cassette into pSPTK01a with PYTK072 (ConL2) and pYTK04 (ConRE) by Golden Gate end-on-digestion.

To construct the pSP-Cas9sgRNA plasmid, primers were designed to amplify pGPD3-Cas9-tADH1 from pSPCO-Cas9 as a single fragment. Next, the sgRNA cassette from IDT was amplified as a second fragment with *Bsa*I recognition sites. Finally, the Cas9 cassette was assembled with the sgRNA cassette into pSPTK01b using Golden Gate cloning (end-on-digestion).

6.15 Analyzing the effect of codon optimization of Cas9 by growth assays.

Plasmids were transformed with an empty vector into wild-type fission yeast strain YZY585. Colonies were inoculated in an overnight culture and diluted to an OD of 0.3 at 595nm for normalization. The cultures were then diluted to 1/100 in 150µL of PMG-URA in triplicates with negative control (growth medium) and positive control (wild type YZY585). Growth was measured on the Biotek Synergy H1 Hybrid Microplate Reader with continuous double orbital shaking at 30ºC. Reads were taken every 10 minutes for 48 hours at a wavelength of 595 nm. The data were processed using GraphPrism.

For spotting assays, colonies were inoculated into an overnight culture and back diluted to an OD of 0.3 at 595nm for normalization. This was followed by 1/10 serial dilutions and spotted using a 96-well plate stamper on an Omni tray with PMG-URA agar for three days at 30ºC.

6.16 Targeting *Ade6* gene using SPCO-Cas9 and SPCO-dCAS9

SPCO-Cas9 and sgRNA plasmids were used to target the *Ade*6 gene. The 20 bp targeting sequence was designed by creating oligos with the protospacer sequence with *Bsm*BI overhangs identical to the sgRNA backbone. The targeting sequence was designed using the CRISPR guide RNA tool in version 11 of Geneious software that screens sgRNAs based on high ON-target and low OFF-target scores [80,81]. The target sequence with a high ON-target efficiency near the 5' end of the gene ensures that upon NHEJ repair will lead to a frame-shift mutation was chosen [81]. The oligos were annealed and assembled into pk101d-sgRNA by *Bsm*BI Golden Gate end-on-digestion method. SPCO-Cas9 and sgRNA^{ade6} plasmids were transformed into YZY585 wild-type strain and plated on PMG-URE-LEU. One red colony was emulsified in 20 mM NaOH and heated for 2 min. The suspension was then centrifuged, and the supernatant was used for colony

PCR with *Accuprime PFX* polymerase. The PCR product was sent for sequencing to confirm the *Ade6* mutation.

6.17 Verification of Plasmid Constructs

All plasmid constructs were validated by restriction enzyme digestion, Sanger sequencing offered by Eurofins or nanopore sequencing offered by Plasmidasaurus.

Chapter 7 - Bibliography

1. Nora LC, Westmann CA, Martins-Santana L, Alves L de F, Monteiro LMO, Guazzaroni M-E, et al. The art of vector engineering: towards the construction of next-generation genetic tools. Microb Biotechnol. 2019;12: 125–147.

2. Malcı K, Watts E, Roberts TM, Auxillos JY, Nowrouzi B, Boll HO, et al. Standardization of Synthetic Biology Tools and Assembly Methods for Saccharomyces cerevisiae and Emerging Yeast Species. ACS Synth Biol. 2022;11: 2527–2547.

3. Chen B, Lee HL, Heng YC, Chua N, Teo WS, Choi WJ, et al. Synthetic biology toolkits and applications in Saccharomyces cerevisiae. Biotechnol Adv. 2018;36: 1870–1881.

4. Zhao Y, Boeke JD. Construction of Designer Selectable Marker Deletions with a CRISPR-Cas9 Toolbox in Schizosaccharomyces pombe and New Design of Common Entry Vectors. G3 . 2018;8: 789–796.

5. Bean BDM, Whiteway M, Martin VJJ. The MyLO CRISPR-Cas9 toolkit: a markerless yeast localization and overexpression CRISPR-Cas9 toolkit. G3 Genes|Genomes|Genetics. 2022;12: jkac154.

6. Lee ME, DeLoache WC, Cervantes B, Dueber JE. A Highly Characterized Yeast Toolkit for Modular, Multipart Assembly. ACS Synth Biol. 2015;4: 975–986.

7. Marillonnet S, Grützner R. Synthetic DNA assembly using Golden Gate cloning and the hierarchical modular cloning pipeline. Curr Protoc Mol Biol. 2020;130: e115.

8. Alberti S, Gitler AD, Lindquist S. A suite of Gateway cloning vectors for high-throughput genetic analysis in Saccharomyces cerevisiae. Yeast. 2007;24: 913–919.

9. Hayden E, Chen S, Chumley A, Xia C, Zhong Q, Ju S. A Genetic Screen for Human Genes Suppressing FUS Induced Toxicity in Yeast. G3 . 2020;10: 1843–1852.

10. Kachroo AH, Laurent JM, Yellman CM, Meyer AG, Wilke CO, Marcotte EM. Systematic humanization of yeast genes reveals conserved functions and genetic modularity. Science. 2015;348: 921–925.

11. Røkke G, Korvald E, Pahr J, Oyås O, Lale R. BioBrick assembly standards and techniques and associated software tools. Methods Mol Biol. 2014;1116: 1–24.

12. Sarrion-Perdigones A, Falconi EE, Zandalinas SI, Juárez P, Fernández-del-Carmen A, Granell A, et al. GoldenBraid: an iterative cloning system for standardized assembly of reusable genetic modules. PLoS One. 2011;6: e21622.

13. Guo Y, Dong J, Zhou T, Auxillos J, Li T, Zhang W, et al. YeastFab: the design and construction of standard biological parts for metabolic engineering in Saccharomyces cerevisiae. Nucleic Acids Res. 2015;43: e88.

14. Botstein D, Fink GR. Yeast: an experimental organism for 21st Century biology. Genetics. 2011;189: 695–704.

15. Scott LH, Wigglesworth MJ, Siewers V, Davis AM, David F. Genetically Encoded Whole Cell Biosensor for Drug Discovery of HIF-1 Interaction Inhibitors. ACS Synth Biol. 2022;11: 3182–3189.

16. Kachroo AH, Vandeloo M, Greco BM, Abdullah M. Humanized yeast to model human biology, disease and evolution. Dis Model Mech. 2022;15. doi:10.1242/dmm.049309

17. Laurent JM, Garge RK, Teufel AI, Wilke CO, Kachroo AH, Marcotte EM. Humanization of yeast genes with multiple human orthologs reveals functional divergence between paralogs. PLoS Biol. 2020;18: e3000627.

18. Hamza A, Driessen MRM, Tammpere E, O'Neil NJ, Hieter P. Cross-Species Complementation of Nonessential Yeast Genes Establishes Platforms for Testing Inhibitors of Human Proteins. Genetics. 2020;214: 735–747.

19. Boonekamp FJ, Knibbe E, Vieira-Lara MA, Wijsman M, Luttik MAH, van Eunen K, et al. Full humanization of the glycolytic pathway in Saccharomyces cerevisiae. Cell Rep. 2022;39: 111010.

20. Sun S, Yang F, Tan G, Costanzo M, Oughtred R, Hirschman J, et al. An extended set of yeast-based functional assays accurately identifies human disease mutations. Genome Res. 2016;26: 670–680.

21. Kitagawa K, Hieter P. Evolutionary conservation between budding yeast and human kinetochores. Nat Rev Mol Cell Biol. 2001;2: 678–687.

22. Garge RK, Laurent JM, Kachroo AH, Marcotte EM. Systematic Humanization of the Yeast Cytoskeleton Discerns Functionally Replaceable from Divergent Human Genes. Genetics. 2020;215: 1153–1169.

23. Kim S, Park J, Kim T, Lee J-S. The functional study of human proteins using humanized yeast. J Microbiol. 2020;58: 343–349.

24. Steinmetz LM, Scharfe C, Deutschbauer AM, Mokranjac D, Herman ZS, Jones T, et al. Systematic screen for human disease genes in yeast. Nat Genet. 2002;31: 400–404.

25. Laurent JM, Young JH, Kachroo AH, Marcotte EM. Efforts to make and apply humanized yeast. Brief Funct Genomics. 2015;15: 155–163.

26. Cervelli T, Galli A. Yeast as a Tool to Understand the Significance of Human Disease-Associated Gene Variants. Genes . 2021;12. doi:10.3390/genes12091303

27. Lamesch P, Li N, Milstein S, Fan C, Hao T, Szabo G, et al. hORFeome v3.1: a resource of human open reading frames representing over 10,000 human genes. Genomics. 2007;89: 307–315.

28. MGC Project Team, Temple G, Gerhard DS, Rasooly R, Feingold EA, Good PJ, et al. The completion of the Mammalian Gene Collection (MGC). Genome Res. 2009;19: 2324–2333.

29. Jo M, Chung AY, Yachie N, Seo M, Jeon H, Nam Y, et al. Yeast genetic interaction screen of human genes associated with amyotrophic lateral sclerosis: identification of MAP2K5 kinase as a potential drug target. Genome Res. 2017;27: 1487–1500.

30. Potapov V, Ong JL, Kucera RB, Langhorst BW, Bilotti K, Pryor JM, et al. Comprehensive Profiling of Four Base Overhang Ligation Fidelity by T4 DNA Ligase and Application to DNA Assembly. ACS Synth Biol. 2018;7: 2665–2674.

31. Storch M, Haines MC, Baldwin GS. DNA-BOT: a low-cost, automated DNA assembly platform for synthetic biology. Synth Biol. 2020;5: ysaa010.

32. Bahassi EM, O'Dea MH, Allali N, Messens J, Gellert M, Couturier M. Interactions of CcdB with DNA Gyrase: INACTIVATION OF GyrA, POISONING OF THE GYRASE-DNA COMPLEX, AND THE ANTIDOTE ACTION OF CcdA*. J Biol Chem. 1999;274: 10936–10944.

33. Reece-Hoyes JS, Walhout AJM. Gateway Recombinational Cloning. Cold Spring Harb Protoc. 2018;2018. doi:10.1101/pdb.top094912

34. Marsischky G, LaBaer J. Many Paths to Many Clones: A Comparative Look at High-Throughput Cloning Methods. Genome Res. 2004;14: 2020–2028.

35. Otto M, Skrekas C, Gossing M, Gustafsson J, Siewers V, David F. Expansion of the Yeast Modular Cloning Toolkit for CRISPR-Based Applications, Genomic Integrations and Combinatorial Libraries. ACS Synth Biol. 2021;10: 3461–3474.

36. Vo TV, Das J, Meyer MJ, Cordero NA, Akturk N, Wei X, et al. A Proteome-wide Fission Yeast Interactome Reveals Network Evolution Principles from Yeasts to Human. Cell. 2016;164: 310–323.

37. Lee MG, Nurse P. Complementation used to clone a human homologue of the fission yeast cell cycle control gene cdc2. Nature. 1987;327: 31–35.

38. Olsson I, Bjerling P. Advancing our understanding of functional genome organisation through studies in the fission yeast. Curr Genet. 2011;57: 1–12.

39. Heinicke S, Livstone MS, Lu C, Oughtred R, Kang F, Angiuoli SV, et al. The Princeton Protein Orthology Database (P-POD): a comparative genomics analysis tool for biologists. PLoS One. 2007;2: e766.

40. Costanzo M, VanderSluis B, Koch EN, Baryshnikova A, Pons C, Tan G, et al. A global genetic interaction network maps a wiring diagram of cellular function. Science. 2016;353. doi:10.1126/science.aaf1420

41. Dixon SJ, Fedyshyn Y, Koh JLY, Prasad TSK, Chahwan C, Chua G, et al. Significant conservation of synthetic lethal genetic interaction networks between distantly related eukaryotes. Proceedings of the National Academy of Sciences. 2008;105: 16653–16658.

42. Ahn J, Choi C-H, Kang C-M, Kim C-H, Park H-M, Song K-B, et al. Generation of expression vectors for high-throughput functional analysis of target genes in Schizosaccharomyces pombe. J Microbiol. 2009;47: 789–795.

43. Vještica A, Marek M, Nkosi PJ, Merlini L, Liu G, Bérard M, et al. A toolbox of stable integration vectors in the fission yeast Schizosaccharomyces pombe. J Cell Sci. 2020;133. doi:10.1242/jcs.240754

44. Forsburg SL, Rhind N. Basic methods for fission yeast. Yeast. 2006;23: 173–183.

45. Hoffman CS, Wood V, Fantes PA. An Ancient Yeast for Young Geneticists: A Primer on the Schizosaccharomyces pombe Model System. Genetics. 2015;201: 403–423.

46. Pancaldi V, Saraç OS, Rallis C, McLean JR, Převorovský M, Gould K, et al. Predicting the fission yeast protein interaction network. G3 . 2012;2: 453–467.

47. Chung K-S, Jang Y-J, Kim N-S, Park S-Y, Choi S-J, Kim J-Y, et al. Rapid screen of human genes for relevance to cancer using fission yeast. J Biomol Screen. 2007;12: 568–577.

48. Tosti E, Katakowski JA, Schaetzlein S, Kim H-S, Ryan CJ, Shales M, et al. Evolutionarily conserved genetic interactions with budding and fission yeast MutS identify orthologous relationships in mismatch repair-deficient cancer cells. Genome Med. 2014;6: 68.

49. Zhao Y, Zurawel AA, Jenkins NP, Duennwald ML, Cheng C, Kettenbach AN, et al. Comparative Analysis of Mutant Huntingtin Binding Partners in Yeast Species. Sci Rep. 2018;8: 9554.

50. Balasubramanian MK, Bi E, Glotzer M. Comparative analysis of cytokinesis in budding yeast, fission yeast and animal cells. Curr Biol. 2004;14: R806-18.

51. Sun Y, Schöneberg J, Chen X, Jiang T, Kaplan C, Xu K, et al. Direct comparison of clathrin-mediated endocytosis in budding and fission yeast reveals conserved and evolvable features. Elife. 2019;8: e50749.

52. Wang K, Okada H, Bi E. Comparative Analysis of the Roles of Non-muscle Myosin-IIs in Cytokinesis in Budding Yeast, Fission Yeast, and Mammalian Cells. Front Cell Dev Biol. 2020;8: 593400.

53. Roux AE, Chartrand P, Ferbeyre G, Rokeach LA. Fission yeast and other yeasts as emergent models to unravel cellular aging in eukaryotes. J Gerontol A Biol Sci Med Sci. 2010;65: 1–8.

54. Murray JM, Watson AT, Carr AM. Molecular Genetic Tools and Techniques in Fission Yeast. Cold Spring Harb Protoc. 2016;2016: db.top087601.

55. Forsburg SL. The art and design of genetic screens: yeast. Nat Rev Genet. 2001;2: 659–668.

56. Raschmanová H, Weninger A, Glieder A, Kovar K, Vogl T. Implementing CRISPR-Cas technologies in conventional and non-conventional yeasts: Current state and future prospects. Biotechnol Adv. 2018;36: 641–665.

57. Ishikawa K, Soejima S, Masuda F, Saitoh S. Implementation of dCas9-mediated CRISPRi in the fission yeast Schizosaccharomyces pombe. G3 Genes|Genomes|Genetics. 2021;11: jkab051.

58. Hofmann A, Falk J, Prangemeier T, Happel D, Köber A, Christmann A, et al. A tightly regulated and adjustable CRISPR-dCas9 based AND gate in yeast. Nucleic Acids Res. 2019;47: 509–520.

59. Jacobs JZ, Ciccaglione KM, Tournier V, Zaratiegui M. Implementation of the CRISPR-Cas9 system in fission yeast. Nat Commun. 2014;5: 5344.

60. Torres-Garcia S, Di Pompeo L, Eivers L, Gaborieau B, White SA, Pidoux AL, et al. SpEDIT: A fast and efficient CRISPR/Cas9 method for fission yeast. Wellcome Open Res. 2020;5: 274.

61. Kim D-U, Hayles J, Kim D, Wood V, Park H-O, Won M, et al. Analysis of a genome-wide set of gene deletions in the fission yeast Schizosaccharomyces pombe. Nat Biotechnol. 2010;28: 617–623.

62. Enghiad B, Xue P, Singh N, Boob AG, Shi C, Petrov VA, et al. PlasmidMaker is a versatile, automated, and high throughput end-to-end platform for plasmid construction. Nat Commun. 2022;13: 1–13.

63. Matsuyama A, Shirai A, Yoshida M. A series of promoters for constitutive expression of heterologous genes in fission yeast. Yeast. 2008;25: 371–376.

64. Siam R, Dolan WP, Forsburg SL. Choosing and using Schizosaccharomyces pombe plasmids. Methods. 2004;33: 189–198.

65. Wang H, Wang H, Wang M, Zhang L, Wang R, Mei Y, et al. Identification and refinement of two strong constitutive promoters for gene expression system of Schizosaccharomyces pombe. World J Microbiol Biotechnol. 2014;30: 1809–1817.

66. Sampaio-Marques B, Felgueiras C, Silva A, Rodrigues M, Tenreiro S, Franssens V, et al. SNCA (α-synuclein)-induced toxicity in yeast cells is dependent on sirtuin 2 (Sir2)-mediated mitophagy. Autophagy. 2012;8: 1494–1509.

67. Brandis KA, Holmes IF, England SJ, Sharma N, Kukreja L, DebBurman SK. alpha-Synuclein fission yeast model: concentration-dependent aggregation without plasma membrane localization or toxicity. J Mol Neurosci. 2006;28: 179–191.

68. Dani GM, Zakian VA. Mitotic and meiotic stability of linear plasmids in yeast. Proc Natl Acad Sci U S A. 1983;80: 3406–3410.

69. Sonnhammer ELL, Östlund G. InParanoid 8: orthology analysis between 273 proteomes, mostly eukaryotic. Nucleic Acids Res. 2015;43: D234-9.

70. Morishita M, Morimoto F, Kitamura K, Koga T, Fukui Y, Maekawa H, et al. Phosphatidylinositol 3-phosphate 5-kinase is required for the cellular response to nutritional starvation and mating pheromone signals in Schizosaccharomyces pombe. Genes Cells. 2002;7: 199–215.

71. Xue-Franzén Y, Kjaerulff S, Holmberg C, Wright A, Nielsen O. Genomewide identification of pheromone-targeted transcription in fission yeast. BMC Genomics. 2006;7: 303.

72. Furuya K, Niki H. Construction of diploid zygotes by interallelic complementation of ade6 in Schizosaccharomyces japonicus. Yeast. 2011;28: 747–754.

73. Ma D, Liu F. Genome Editing and Its Applications in Model Organisms. Genomics Proteomics Bioinformatics. 2015;13: 336–344.

74. Fu H, Liang Y, Zhong X, Pan Z, Huang L, Zhang H, et al. Codon optimization with deep learning to enhance protein expression. Sci Rep. 2020;10: 1–9.

75. Wu X, Kriz AJ, Sharp PA. Target specificity of the CRISPR-Cas9 system. Quant Biol. 2014;2: 59–70.

76. Scott WG, Horan LH, Martick M. The hammerhead ribozyme: structure, catalysis, and gene regulation. Prog Mol Biol Transl Sci. 2013;120: 1–23.

77. Zhao Y, Boeke JD. CRISPR-Cas12a system in fission yeast for multiplex genomic editing and CRISPR interference. Nucleic Acids Res. 2020;48: 5788–5798.

78. Ng H, Dean N. Dramatic Improvement of CRISPR/Cas9 Editing in Candida albicans by Increased Single Guide RNA Expression. mSphere. 2017;2. doi:10.1128/mSphere.00385-16

79. Liu J, Chang W, Pan L, Liu X, Su L, Zhang W, et al. An Improved Method of Preparing High Efficiency Transformation Escherichia coli with Both Plasmids and Larger DNA Fragments. Indian J Microbiol. 2018;58: 448–456.

80. Kearse M, Moir R, Wilson A, Stones-Havas S, Cheung M, Sturrock S, et al. Geneious Basic: an integrated and extendable desktop software platform for the organization and analysis of sequence data. Bioinformatics. 2012;28: 1647–1649.

81. Doench JG, Fusi N, Sullender M, Hegde M, Vaimberg EW, Donovan KF, et al. Optimized sgRNA design to maximize activity and minimize off-target effects of CRISPR-Cas9. Nat Biotechnol. 2016;34: 184–191.

Supplementary Information

Table S.1 Table of plasmids generated in this study

Plasmid	Antibiotic	Marker	Description
pSPTK01a	CamR	Ura4	Direct Cloning vector with BsaI sites
pSPTK01b	AmpR	Ura4	Direct Cloning vector with BsmBI sites
pSPTK01c	AmpR	Leu3	Direct Cloning vector with BsaI sites
pSPTK02a	AmpR	Ura4	Direct Cloning vector with BsaI and BsmBI sites and GFP dropout
pSPTK02b	AmpR	Ura4	Direct Cloning vector with BsaI sites and GFP dropout
pSPTK02c	AmpR	Leu3	Direct Cloning vector with BsaI sites and GFP dropout
pSPRC03a	CamR/AmpR	Ura4	Direct Cloning vector with BsaI, BsmbI, attb sites and ccdB dropout
pSPRC03b	CamR/AmpR	Leu3	Direct Cloning vector with pGPD3, BsaI, attb sites and ccdB dropout
pSPTK04a	CamR		Part vector for pADH1 with BsaI sites
pSPTK04b	CamR		Part vector for pENO101with BsaI sites
pSPTK04c	CamR		Part vector for pGPD3 with BsaI sites
pSPTK04d	CamR		Part vector for pZ3EV with BsaI sites
pSPTK05a	CamR		Part vector for tADH1 with BsaI sites
pSPTK05b	CamR		Part vector for tCYC1 with BsaI sites
pSPRC06a	CamR/AmpR	Ura4	Expression vector with pGPD3, ccdB-egfp, and BsaI, attb sites
pSPRC06b	CamR/AmpR	Ura4	Expression vector with pENO101, ccdB-egfp and BsaI, attb sites
pSPRC06c	CamR/AmpR	Ura4	Expression vector with pADH1, ccdB-egfp and BsaI, attb sites
pSPRC06d	CamR/AmpR	Ura4	Expression vector with pADH1, ccdB-egfp and BsaI, attb sites
pSPCO-Cas9	AmpR	Ura4	Expression vector with pGPD
pSPCO-dCas9	AmpR	Ura4	Expression vector with pGPD
pSP-sgRNA	AmpR	Leu3	Expression vector with sgRNA cassette
pSP-Cas9sgRNA	AmpR	Ura4	Cas9sgRNA Expression vector with BsmBI sites and GFP dropout
pSCRC083	AmpR/CamR		Direct Cloning vector with BsaI sites and ccdB dropout
pSCRC084	KanR/CamR		Direct Cloning vector with BsaI sites and ccdB dropout
pSCRC085	SpecR/CamR		Direct Cloning vector with BsaI sites and ccdB dropout
pSCRC089	AmpR/CamR		Direct Cloning vector with BsaI sites and ccdB dropout
pSCRC090	KanR/CamR		Direct Cloning vector with BsaI sites and ccdB dropout
pSCRC091	SpecR/CamR		Direct Cloning vector with BsaI sites and ccdB dropout
pSCRC095	AmpR/CamR		Direct Cloning vector with BsaI sites and ccdB dropout
pSCRC096	KanR/CamR		Ura 3 Integration vector with BsaI sites and ccdB dropout
pSCRC097	KanR/CamR		Leu2 Integration vector with BsaI sites and ccdB dropout
pSCRCCas901	KanR/CamR	kanMX	Cas9sgRNA expression vector with BsaI sites and ccdB dropout
pSCRCCas902	KanR/CamR	Ura3	Cas9sgRNA expression vector with BsaI sites and ccdB dropout
pSCRCCen01	KanR/CamR	Ura3	Expression vector with BsmBI, BsaI sites and ccdB dropout
pSCRCFgf16	KanR	NAT	Fgf16 integration vector with BsaI, BsmbI sites and GFP dropout
pSCRCFgf18	KanR	NAT	Fgf18 integration vector with BsaI, BsmbI sites and GFP dropout
pSCRCFgf19	KanR	NAT	Fgf19 integration vector with BsaI, BsmbI sites and GFP dropout
pSCRCFgf21	KanR	NAT	Fgf21 integration vector with BsaI, BsmbI sites and GFP dropout
pSCRCFgf24	KanR	NAT	Fgf24 integration vector with BsaI, BsmbI sites and GFP dropout

Table S.2 Table of primers generate in this study

Gene	Name	Type	Sequence
sequencing	pk101a cloning site FP	Fp	AGATGAATGTAAAATACCATGTAGA
	pk101a cloning site RP	Rp	AATTACAACAGTACTGCGATGAG
sequencing	Pk101c cloning site FP	Fp	CGTCTCTGTTCTAATGTAAAATTTTTTTGGTTGGTTATTGAAAAAGTC
	Pk101c cloning site RP	Rp	AGGCAACTATGGATGAACGAAA
sequencing	Pk101d cloning site FP	Fp	GGTCTCATGTACCGGTGCTTGAGACGGGCCCGTCTCATCAGCAACTCGGTCATAAAGTTGAAC
	Pk101d cloning site RP	Rp	AGGCAACTATGGATGAACGAAA
URA4	URA FP	Fp	CGTCTCTGTTCTAATGTAAAATTTTTTTGGTTGGTTATTGAAAAAGTC
	URA RP	Rp	CGTCTCTCATCAACTTTGCTTTTAAACCTTTAATTTCGATCCAA
LEU1	LEU FP	Fp	GGTCTCTCCAATATATATATTAATTTACAATGAGTGTCAGAT
	LEU RP	Rp	GTTCAACTTTATGACCGAGTTGCTGATGAGACGGGCCCGTCTCAAGCACCGGTACATGAGACC
ARS1	Ars1 FP	Fp	CGTCTCTTCGGTTGTACGTCCTTGGGAGTCCG
	Ars1 RP	Rp	CGTCTCATTGGGGGATTTGTAGCTAAGCTCATCG
eGFP	GFP (Bsa1 and Bsmb1) FP	Fp	ATGCCTGAAGAGACGACAATTGAGACCGAAAGTGAAACGTGATTTCATGC
	GFP (Bsa1 and Bsmb1) RP	Rp	ATGCTGCTAGAGACGTTCGGTGAGACCTATAAACGCAGAAAGGCCCAC
eGFP	Pk101d+egfp FP	Fp	CCCTAGAGACGAAACGTGAGACCGAAAGTGAAACGTGATTTCATGC
	Pk101d+egfp RP	Rp	TGTAAGAGACGTCAGCTGAGACCTATAAACGCAGAAAGGCCCAC
ccdB	Pk101d+ccdb FP	Fp	TATGTGAGACCAACTAGTGGATCCCCCATCACAA
	Pk101d+ccdb RP	Rp	GGATTGAGACCTCACCACTTTGTACAAGAAAGCTGAA
eGFP	Pk101f GFP (Bsa1) FP	Fp	GATCCGTCTCTCTGACGAACGTGAGACCGAAAGTGAAACGTGATTTCATGC
	Pk101f GFP (Bsa1) RP	Rp	GATCCGTCTCTTGCTGCCAGCTGAGACCTATAAACGCAGAAAGGCCCAC
ccdB	Pk101e ccdB FP	Fp	GATCGGTCTCATATGCCCAGCGGCCG
	Pk101e ccdB RP	Rp	GATCGGTCTCAGGATCAGCCCATCACCACTTTG
ccdB-eGFP	Pk101k ccdB-eGFP FP	Fp	GATCGGTCTCATATGCCCAGCGGCCG
	Pk101k ccdB-eGFP-RP	Rp	ATGGACGAGCTGTACAAGTAAATCCTGAGACCGATC
ADH1	pADH1 FP	Fp	GCATCGTCTCATCGGTCTCAAACGGCCCTACAACAACTAAGAAAATGGC
	pADH1 RP	Rp	ATGCCGTCTCAGGTCTCACATAAATTCTCTTGCTTAAAGAAAAGCGAAGGC
ENO101	pENO101 FP	Fp	GCATCGTCTCATCGGTCTCAAACGTGCCCCTTCTAAGCTCG
	pENO101 RP	Rp	AGTATTCTACAGTAAACATCGTTAATCTATGTGAGACCTGAGACGGCAT
GPD3	pGPD3 FP	Fp	GCATCGTCTCATCGGTCTCAAACGCGATTGTTGTATGATTATGAGCC
	pGPD3 RP	Rp	ATGCCGTCTCAGGTCTCACATATGTTATCTGAAAAGAGTTAGTAAGAAG
Z3EV	pZ3EV FP	Fp	GCATCGTCTCATCGGTCTCAAACGGTTATATTGAATTTTCAAAAATTCTTACTTTTTT
	pZ3EV RP	Rp	ATGCCGTCTCAGGTCTCACATATATAGTTTTTTCTCCTTGACGTTAAAG
cassette	GPD-CAS9-TADH1 FP pk101c	Fp	CACCACAGGTCTCGCTGACGATTGTTGTATGATTATGAGCCAAAAATAT
	GPD-CAS9-TADH1 RP pk101c	Rp	CGCTAGGGATAACAGGGTAATATGATGCGAGACCTGTGGTG
cassette	sgRNA cassette FP pk101c	Fp	CACCACAGGTCTCGGATGTTTGCTTATGTTGGTGGTAGTTGG
	sgRNA cassette RP pk101c	Rp	CACCACAGGTCTCGTGTATTCAAAAAAACCCAAAAAAATTATTTAACAAAAAGG
PRE4	Pre4 FP	Fp	GTGCGCAAGTTTGTACAAAAAAGCAGGCTTGATGAGTTTTTTAGAATTAACAGAGGTTT
	Pre4 RP	Rp	ATACACCACTTTGTACAAGAAAGCTGGGTGGTTATACGGTTTGAGTCCCGTAA
PRE8	Pre 8 FP	Fp	GTGCGCAAGTTTGTACAAAAAAGCAGGCTTGATGACTGATAAATACGCGTTCTC
	Pre8 RP	Rp	ATACACCACTTTGTACAAGAAAGCTGGGTGGTTATACTTGGTCGAGATAATCACG
ADE6	Ade 6 sgrna1 FP	Fp	AGAAATTGGGCCGAATGATGGTAG
	Ade 6 sgrna1 RP	Rp	AGAAGCGCACCGCATCCATGGCAA
	Ade6 confirmation FP	Fp	CAACTTGGTGGTGAGGTAAACG
	Ade6 confirmation RP	Rp	CAACTACATCTTTTAATAATTGAAGAC

Figure S.1: Methods to assemble RoboClo Vectors

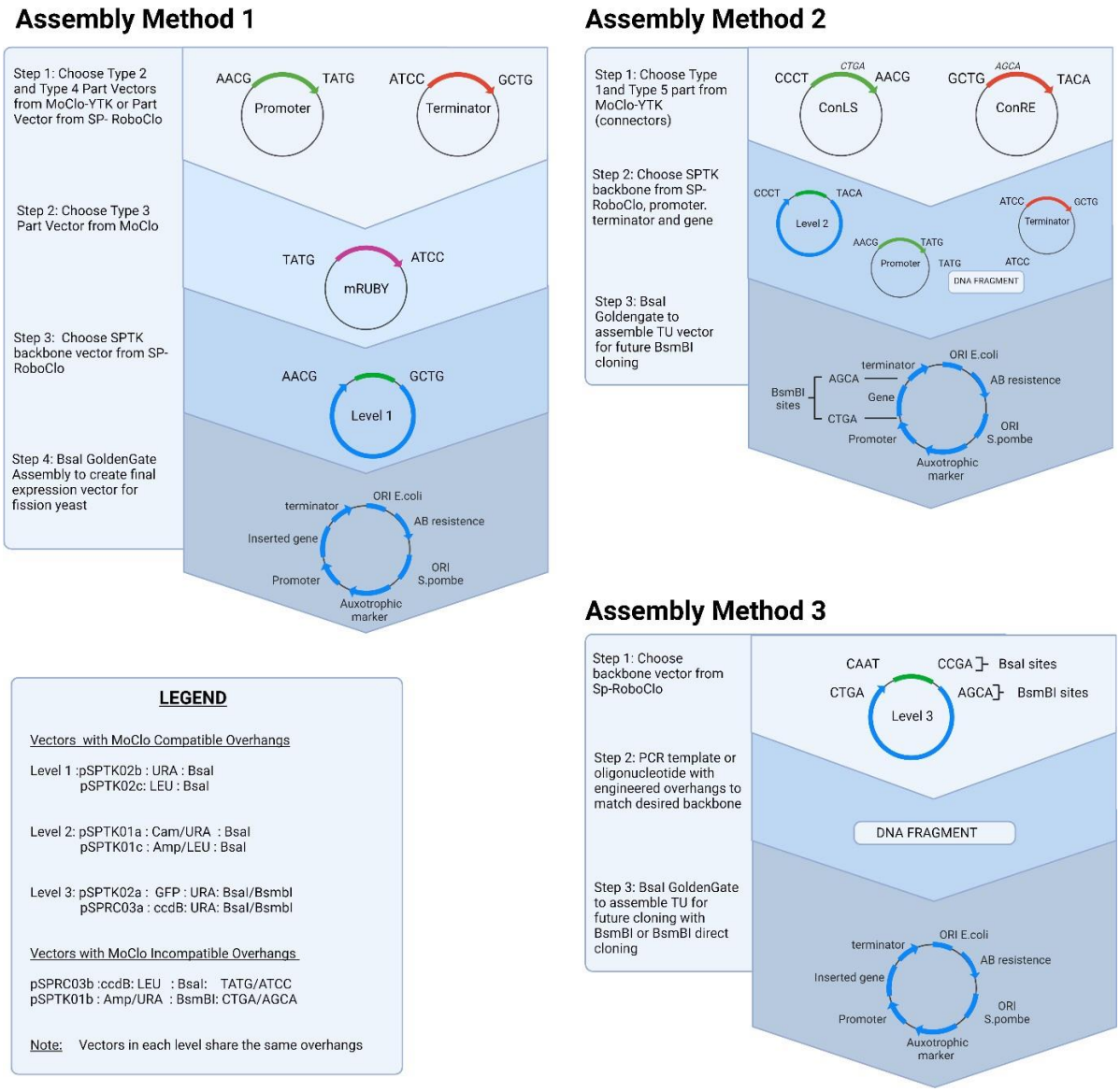

LEGEND

Vectors with MoClo Compatible Overhangs

Level 1 :pSPTK02b : URA : BsaI
pSPTK02c: LEU : BsaI

Level 2: pSPTK01a : Cam/URA : BsaI
pSPTK01c : Amp/LEU : BsaI

Level 3: pSPTK02a : GFP : URA: BsaI/BsmbI
pSPRC03a : ccdB: URA: BsaI/BsmbI

Vectors with MoClo Incompatible Overhangs

pSPRC03b :ccdB: LEU : BsaI: TATG/ATCC
pSPTK01b : Amp/URA : BsmBI: CTGA/AGCA

Note: Vectors in each level share the same overhangs